

SHAKING TABLE DYNAMICS: RESULTS FROM A TEST-ANALYSIS COMPARISON STUDY

TOMASO L. TROMBETTI*

*Facoltà di Ingegneria, Dip. D.I.S.T.A.R.T., Università' degli Studi di Bologna,
v. Risorgimento 2, 40136 Bologna, Italy
tomtr@rice.edu*

JOEL P. CONTE†

*University of California at San Diego, Department of Structural Engineering,
9500 Gilman Drive, La Jolla, California, USA
jpconte@ucsd.edu*

Received 1 October 2001

Revised 3 June 2002

Accepted 8 June 2002

This paper presents the results of a comprehensive comparison study between the analytically predicted and experimentally identified dynamics of the shaking table system built recently in the Structural Engineering Laboratory at Rice University in Houston, Texas. The primary objectives of the research presented here are two-fold: (1) to shed light into the dynamic performance of a small-to-medium size, uni-axial, servo-hydraulic, displacement-controlled shaking table system, and (2) to validate a linearised dynamic model of the system (in the form of the total shaking table transfer function) developed earlier by the authors from basic principles. The analytical model incorporates the inherent dynamic characteristics of the various components of the shaking table system (i.e. controller, servovalve, actuator, test specimen, and reaction mass) and their dynamic interaction.

The test-analysis correlation study performed over a wide range of operating and payload conditions provides useful information on the sensitivity of the shaking table transfer function to control gain parameters and how it can be used to tune the shaking table controller for optimum performance under various payload conditions. The good test-analysis correlation results obtained validate the analytical shaking table model, show its robustness, and provide keen insight into the underlying coupled dynamics of a shaking table system. In order to achieve this good test-analysis correlation, it was crucial to include a time delay in the analytical model of the shaking table system (innovative feature of the model to account for the time lag in the response of the servovalve-actuator system). The expected significant dynamic interaction between payload and shaking table is also confirmed by this study.

Keywords: Servo-hydraulic shaking table; test-analysis comparison; servovalve-actuator-control-foundation-specimen interaction; transfer function sensitivity; servovalve time delay.

*Assistant Professor; formerly Graduate Student at Rice University, Houston, Texas, USA.

†Associate Professor; formerly at the University of California at Los Angeles (1998–2001) and at Rice University, Houston, Texas (1990–1997), Corresponding author.

1. Introduction

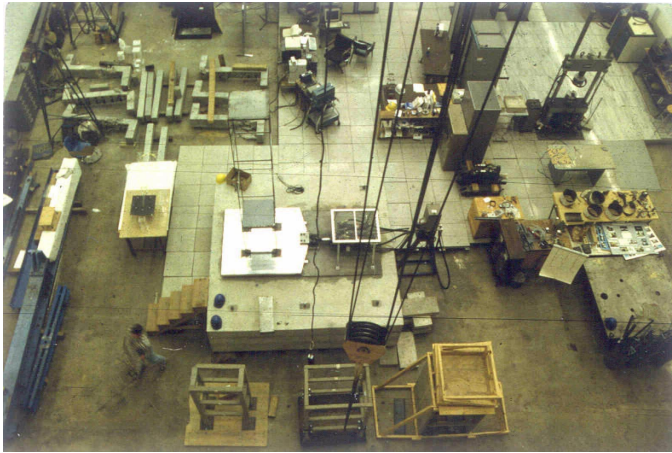
It is known that the reproduction through shaking table of commanded dynamic signals (e.g. earthquake ground motions) remains imperfect [Rea *et al.*, 1977; Hwang *et al.*, 1987; Rinawi and Clough, 1991]. The undesired signal distortion depends on the inherent dynamic characteristics of the various sub-systems (mechanical, hydraulic, and electronic) of the shaking table — payload system and their interaction. In the past decade, significant research was devoted to both evaluating the actual performance of existing shaking table facilities [Clark, 1992; Kusner *et al.*, 1992; Carydis *et al.*, 1995; Crewe and Severn, 2001] and developing advanced (real-time adaptive) control algorithms to improve the accuracy in time history reproduction [Stoten and Gomez, 2001].

In order to achieve meaningful and reliable results in performing dynamic tests with a shaking table, a mere evaluation of the accuracy of the table in motion reproduction is not sufficient. Indeed, to effectively use a shaking table for structural dynamic testing, it is necessary to identify and understand the unavoidable dynamic interaction between the several sub-systems (mechanical, hydraulic, and electronic) of the shaking table — test structure system. Furthermore, a thorough understanding of the sensitivities of the shaking table dynamics to control parameters/gains provides invaluable guidance in determining the optimal control gain setting that maximises the table accuracy in motion reproduction for a given payload. A complete and reliable understanding of the shaking table dynamics can be obtained only through an in-depth test-analysis correlation study, which is the main focus of this paper.

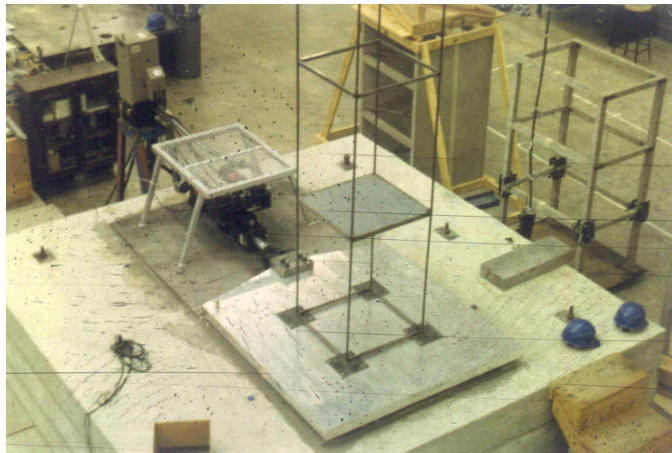
The first part of the paper briefly describes (1) the characteristics of the shaking table system, (2) the linear analytical model used to predict the shaking table dynamics, (3) the method used to estimate the actual shaking table transfer function from dynamic experimental data, and (4) the determination of the unknown (not physically identifiable *a priori*) model parameters based on experimental results in order to properly calibrate the analytical model. The dynamic shaking table model was developed earlier by the authors [Trombetti *et al.*, 1997a; Conte and Trombetti, 2000]. It incorporates the inherent dynamic characteristics of the various components of the shaking table system (i.e. controller, servovalve, actuator, test specimen, and reaction mass) and their dynamic interaction. The second part of the paper presents the results of an exhaustive comparison study between the analytically predicted and experimentally identified shaking table transfer functions for a wide range of operating and payload conditions. The experimental results were obtained by the authors from the uni-axial, servo-hydraulic, stroke controlled shaking table recently built in the Structural Engineering Laboratory of the Civil Engineering Department at Rice University in Houston, Texas. This test-analysis correlation study also serves the purpose of validating the analytical model and evaluating its robustness, another objective of this paper.

2. The Rice University Shaking Table

The Rice University uni-directional shaking table shown in Fig. 1 is capable of reproducing, after scaling for similitude, earthquake ground motions with a peak acceleration up to $6g$'s, a peak velocity up to 90 cm/s (36 in/s), and a peak displacement up to 7.5 cm (3 in), for a maximum payload of 700 kg (1500 lbs). The Rice table has a frequency bandwidth of approximately 70 Hz (for bare table condition). The 150 cm by 150 cm (5 ft by 5 ft) and 7.6 cm (3 in) thick aluminium table platform rides on high precision rails through low friction linear bearings and is driven by a



(a)



(b)

Fig. 1. Rice University shaking table: (a) general configuration, and (b) close-up.

156 kN (35 kips) linear hydraulic actuator powered by a 114 l/min (30 gpm) hydraulic pump. The rail-table system is mounted on a 31850 kg (70 000 lbs) reaction mass consisting of three layered 366 cm × 366 cm × 30.5 cm (12 ft × 12 ft × 1 ft) reinforced concrete slabs post-tensioned together and connected to the laboratory floor through a grid of steel *I*-beams. The hydraulic actuator is driven by a three-stage servovalve governed by a digitally supervised analog controller that employs a proportional-integral-derivative-feedforward-differential pressure algorithm in order to control the displacement of the actuator arm. Feedback signals are provided by an actuator mounted LVDT monitoring the displacement of the actuator arm, a servovalve mounted LVDT monitoring the actual position of the third stage (main stage) spool of the servovalve and one differential pressure (ΔP) transducer monitoring the differential pressure across the actuator piston. Further information and details concerning the analysis, design, and construction of the Rice University shaking table are presented in a comprehensive report by Muhlenkamp *et al.* [1997].

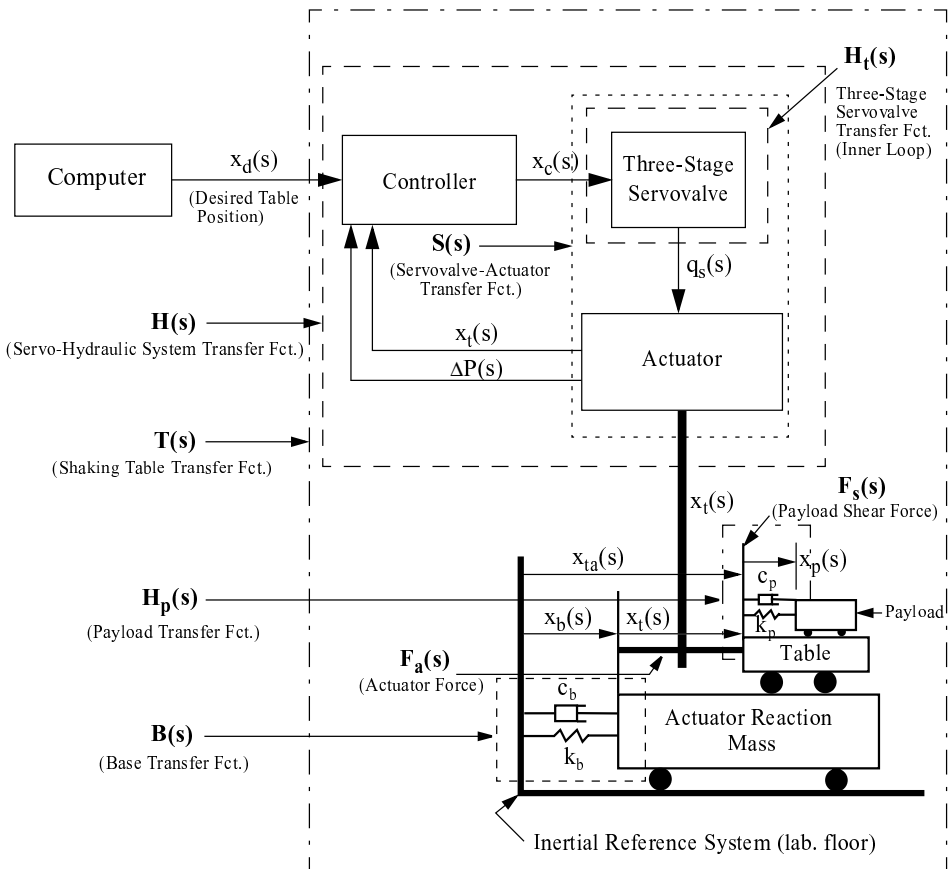


Fig. 2. Pseudo block diagram representation of the shaking table system.

3. Analytical Shaking Table Transfer Function Model

The analytical linear^a dynamic model of the Rice University shaking table used herein was developed earlier by the authors [Trombetti *et al.*, 1997a; Conte and Trombetti, 2000]. It accounts for proportional, integral, derivative, feed-forward, and differential pressure control gains, time delay in the response of the servovalve main stage spool to a given electrical signal, compressibility of the actuator fluid, oil leakage across the sealed joints within the actuator, flexibility of the reaction/foundation mass (or base flexibility), and dynamic characteristics of the test specimen. In other words, this model accounts for the dynamic interaction between the various components of the shaking table system (i.e. controller, servovalve, actuator, test specimen, and reaction mass). Based on the pseudo block diagram representation of the shaking table system shown in Fig. 2, the analytical model of the shaking table system was developed as an input-output transfer function, $T(s)$, in the Laplace domain.^b The input consists of the desired/commanded displacement signal $x_d(t)$ representing the absolute (or total) displacement time history to be reproduced on the shaking table, while the output corresponds to the actual or achieved table absolute (or total)^c displacement response $x_{ta}(t)$. The shaking table transfer function is given by [Conte and Trombetti, 2000]

$$T(s) = \frac{x_{ta}(s)}{x_d(s)} = \frac{x_b(s) + x_t(s)}{x_d(s)} = H(s) \cdot (B(s) + 1) \quad (1)$$

where

$$H(s) = \frac{x_t(s)}{x_d(s)} = \frac{S(s) \cdot [(P_{\text{gain}} + \frac{1}{s} \cdot I_{\text{gain}}) \cdot K_{x\text{-cond}} + s \cdot (FF_{\text{gain}} + D_{\text{gain}}) \cdot K_{D\text{-cond}}]}{1 + S(s) \cdot [(P_{\text{gain}} + \frac{1}{s} \cdot I_{\text{gain}}) \cdot K_{x\text{-cond}} + s \cdot D_{\text{gain}} \cdot K_{D\text{-cond}} - dP_{\text{gain}} \cdot \frac{s^2 \cdot m_t}{A} \cdot K_{dp\text{-cond}} \cdot H_F(s)]} \quad (2)$$

$$S(s) = \frac{x_t(s)}{x_c(s)} = \frac{H_t(s)}{s^3 \cdot \frac{V m_t}{4\beta A} \cdot H_F(s) + s^2 m_t \cdot k_{le} \cdot H_F(s) + s \cdot A} \quad (3)$$

$$H_t(s) = \frac{q_s(s)}{x_c(s)} = k_t \cdot \frac{K_{\text{pro}}^i + s \cdot K_{\text{der}}^i}{1 + A_i(s) \cdot k_1 \cdot k_2 \cdot (K_{\text{pro}}^i + s \cdot K_{\text{der}}^i) e^{-\tau \cdot s}} \cdot e^{-\tau \cdot s} \quad (4)$$

$$H_F(s) = [1 + B(s)] \cdot \left[1 + \frac{m_p}{m_t} \cdot H_p(s) \right] \quad (5)$$

^aEven though servo-hydraulic actuation systems are inherently nonlinear, especially for large amplitude simulations near the performance capacity of the system, linearised models are quite effective in capturing the actual shaking table dynamic behavior as will be shown in this paper.

^bThe expression for the table transfer function $T(f)$ in terms of the cyclic frequency f in Hertz is then simply obtained by using the substitution $s = i2\pi f$ (where $i = \sqrt{-1}$) in the table transfer function expressed in terms of the Laplace parameter s .

^cWith respect to an inertial reference system. In this analytical model, the laboratory ground floor was assumed to be an inertial reference system.

$$B(s) = \frac{x_b(s)}{x_t(s)} = \frac{-s^2 \cdot \frac{m_t}{m_T} \cdot \left\{ 1 + \frac{m_p}{m_t} [H_p(s)] \right\}}{s^2 \left\{ 1 + \frac{m_p}{m_T} \cdot H_p(s) \right\} + s \cdot 2\xi_b\omega_b + \omega_b^2} \quad (6)$$

$$H_p(s) = \frac{x_{ta}(s) + x_p(s)}{x_{ta}(s)} = \frac{s \cdot 2\xi_p\omega_p + \omega_p^2}{s^2 + s \cdot 2\xi_p\omega_p + \omega_p^2}. \quad (7)$$

The system variables entering the above formulation of the shaking table transfer function are defined as follows:

P_{gain} (V/V), I_{gain} (Hz), D_{gain} (s), FF_{gain} (s), dP_{gain} (V/V) = proportional, integral, derivative, feed-forward, and delta-pressure control gains,^d respectively, of the outer control loop; $K_{x\text{-cond}}$, $K_{D\text{-cond}}$ = displacement transducer conditioning/conversion constant (V/m), $K_{dp\text{-cond}}$ = pressure transducer conditioning/conversion constant (V/Pa); m_t = mass of the table platform (including the mass of the moving parts of the servovalve-actuator system); m_b = effective foundation/reaction mass; m_p = mass of test specimen (or payload); $m_T = m_b + m_t$; A = effective cross-sectional area of the actuator piston; V = total volume of both chambers of the actuator; β = effective bulk modulus of the actuator fluid; k_{le} = flow-force fluid leakage coefficient; k_t = table gain factor; K_{pro}^i , K_{der}^i = proportional and derivative gain constants, respectively, of the inner control loop; $A_i(s)$ is the so-called “inner loop” feedback transfer function (or feedback conditioner); τ = servovalve time delay (used to model the time lag in the response of the servovalve-actuator system); ω_b and ξ_b = effective natural circular frequency and damping ratio, respectively, of the reaction/foundation mass;^e ω_p and ξ_p = natural circular frequency and damping ratio, respectively, of the SDOF test specimen. The above shaking table transfer function model for an SDOF payload was also extended to account for a two-dimensional frame-type MDOF test structure. For the sake of conciseness, the model for MDOF payload, although used in this study, is not presented here, but can be found elsewhere [Trombetti *et al.*, 1997a; Conte and Trombetti, 2000]. For the definition of the remaining variables, the reader is referred to Fig. 2.

As the servovalve can be driven much more accurately than the other components (hydraulic and mechanical) of the shaking table system (a fact that was observed experimentally by the authors for the Rice University shaking table), the effect of the inner control loop is usually successfully neglected in shaking table modelling [Rea *et al.*, 1977; Rinawi and Clough, 1991; Dyke *et al.*, 1995]. This can

^dThe notation used in this paper for the control gain parameters differs from that used in the previous paper by the authors [Conte and Trombetti, 2000]. The two notations are related through: $K_{\text{pro}} = P_{\text{gain}} \cdot K_{x\text{-cond}}$, $K_{\text{int}} = I_{\text{gain}} \cdot K_{x\text{-cond}}$, $K_{\text{der}} = D_{\text{gain}} \cdot K_{D\text{-cond}}$, $K_{ff} = FF_{\text{gain}} \cdot K_{D\text{-cond}}$, $K_{dp} = dP_{\text{gain}} \cdot K_{dp\text{-cond}}$. Furthermore, we have that: $K_{\text{pro}} \cdot k_t$ (in previous paper) = $P_{\text{gain}} \cdot K_{x\text{-cond}} \cdot k_t$ (in this paper). The different notation was adopted here in order to be consistent with the user-set control gains adjustable from the front panel of the actual controller.
^e $\omega_b = k_b/(m_b + m_t)$ and $\xi_b = c_b/2\sqrt{k_b(m_b + m_t)}$ where k_b and c_b denote the effective stiffness and effective damping coefficients, respectively, of the reaction/foundation mass.

be achieved by setting $K_{\text{pro}}^i = 1$, $K_{\text{der}}^i = A_i(s) = 0$, thus leading to the following simplified expression for the three-stage servovalve transfer function adopted herein:

$$H_t(s) = \frac{q_s(s)}{x_c(s)} = k_t e^{-\tau s}. \quad (8)$$

The above analytical shaking table model does not account for sensor dynamics as the frequency response of the feedback sensors used by the controller of the Rice University shaking table is flat (i.e. constant amplitude and zero phase) well beyond the operating frequency range of the table (0–80 Hz).

4. Estimation of Actual Shaking Table Transfer Function

To compare the actual performance of the shaking table system with the prediction obtained from the above analytical model, it is necessary to determine the actual total table transfer function from experimental dynamic measurements. Therefore, a transfer function estimation stage must be introduced, which brings in some uncertainty. In order to minimise the uncertainty introduced by this estimation stage, a random excitation approach was used in conjunction with the Bartlett's procedure of spectral estimation [Bartlett, 1948], both briefly described below.

In the case of a linear, time-invariant dynamic system subjected to stochastic/random excitation $F(t)$, an input-output relationship can be expressed in the frequency domain as [Lin, 1986]

$$\Phi_{FX}(\omega) = \Phi_{FF}(\omega) \cdot T(\omega) \quad (9)$$

where ω denotes the circular frequency in rad/sec, $X(t)$ represents the stochastic dynamic response/output of the system, $\Phi_{FF}(\omega)$ and $\Phi_{FX}(\omega)$ are the power spectral density function of the input process and the cross-power spectral density function of the input and output processes, respectively, and $T(\omega)$ is the system transfer function.

In the estimation of the actual shaking table transfer function, the input $F(t)$ and output $X(t)$ are signals in digital form and of limited duration (i.e. time series). Therefore, from these input and output time series, only an imperfect estimation of their power and cross-power spectral density functions can be obtained. Herein, periodogram estimates of $\Phi_{FF}(\omega)$ and $\Phi_{FX}(\omega)$, denoted as $\hat{\Phi}_{FF}(\omega)$ and $\hat{\Phi}_{FX}(\omega)$, respectively, are used.

In order to reduce the inherent statistical variability (i.e. variance) of the periodogram estimate, the Bartlett's procedure of spectral estimation is adopted, which is a non-parametric system identification method. The Bartlett's procedure consists of segmenting the total input and output time series of length L into K segments of equal length M (i.e. $L = KM$). Then, the Bartlett's estimates of $\Phi_{FF}(\omega)$ and $\Phi_{FX}(\omega)$, denoted as $\hat{\Phi}_{FF}^B(\omega)$ and $\hat{\Phi}_{FX}^B(\omega)$, respectively, are obtained by averaging

the corresponding periodogram estimates obtained from each of the K segments, i.e.

$$\hat{\Phi}_{FF}^B(\omega) = \frac{1}{K} \cdot \sum_{j=1}^K \hat{\Phi}_{FF}^{(j)}(\omega), \quad \hat{\Phi}_{FX}^B(\omega) = \frac{1}{K} \cdot \sum_{j=1}^K \hat{\Phi}_{FX}^{(j)}(\omega) \quad (10)$$

where $\hat{\Phi}_{FF}^{(j)}(\omega)$ and $\hat{\Phi}_{FX}^{(j)}(\omega)$ denote the periodogram estimate of the power and cross-power spectral density functions, respectively, computed from the j th time segment (or window).^f

After extensive numerical simulation based on ARMA processes [Trombetti *et al.*, 1997b], the following specific features of the Bartlett’s procedure to estimate the actual total shaking table transfer function between the commanded, $F(t)$, and the actual, $X(t)$, absolute table acceleration were selected. A set of eleven (i.e. $K = 11$) statistically independent, uniformly distributed, discrete white noise realizations of 4.0906 s ($= 2^{14}/4000$) duration output at 4000 Hz were used as commanded table absolute acceleration $F(t)$ with special provisions being made [Trombetti *et al.*, 1997b] to eliminate the transient (nonstationary) part of both commanded, $F(t)$, and actual (recorded), $X(t)$, table acceleration histories. Furthermore, a 3-terms Blackman Harris tapered window was applied to each input and output data segment.^g

For consistency, the commanded displacement (= double integrated commanded white noise acceleration) and achieved table displacement and acceleration were acquired at 4000 Hz sampling frequency and in records of length 2^{14} through the same data acquisition (DAQ) board before being used to estimate the actual shaking table transfer function.^h Given the high sampling rate capability of the dynamic data acquisition boards used in this study and the performance characteristics of their built-in analog and digital anti-aliasing filters, no appreciable signal distortion occurs in the frequency range of interest (0–120 Hz) due to either low-pass filtering or digitisation. The DAQ boards used adjust automatically their cut-off frequency to half the sampling frequency (= Nyquist frequency).

^fThe periodogram estimate of the cross-power spectral density function $\Phi_{RS}^{(j)}(\omega)$ of generic random processes $R(t)$ and $S(t)$ is defined as

$$\hat{\Phi}_{RS}^{(j)}(\omega) = \frac{1}{M} \cdot \left[\overline{R_M^{(j)}(\omega)} \cdot S_M^{(j)}(\omega) \right] \text{ with } R_M^{(j)}(\omega) = \sum_{n=0}^{M-1} w(n) \cdot r((j-1) \cdot M + n) \cdot e^{-i \cdot \omega \cdot n \cdot \Delta t}$$

where the overline denotes the complex conjugate, $w(\dots)$ is the time window (or taper) used to extract the time segments from the total time series $r(\dots)$, and Δt is the sampling time interval.
^gThrough ARMA simulation, this window was found to be optimum for the present application in terms of bias of the spectral estimate and spectral leakage [Trombetti *et al.*, 1997b].

^hThe selected sampling rate ($f_s = 400$ Hz) and number ($N = 2^{14}$) of acquired data samples per record were, respectively, the smallest sampling frequency and largest number of acquired data points, respectively, imposed by the capabilities of the dynamic data acquisition boards and host computer available at the time of this research project at Rice University. Nonetheless, this non-ideal choice of f_s and N (resulting in a relatively large frequency resolution of $\Delta f = 0.24$ Hz) was still deemed acceptable for the purpose of estimating experimentally the total table (with and without specimen) transfer function in the frequency range from 0 to 120 Hz.

5. Determination of Unknown Model Parameters Based on Experimental Results

5.1. Shaking table model parameters

The analytical model of the total shaking table transfer function presented in Sec. 3 depends on a set of parameters which can be subdivided into the following four categories:

- (1) *Known system parameters:* These parameters relate to geometric and physical properties of the system, which are precisely known *a priori*. They are: $A = 82.13 \text{ cm}^2$ (12.73 in²), $V = 1668.86 \text{ cm}^3$ (101.84 in³), $m_t = 643 \text{ kg}$ (1413 lbs), and $m_b = 29\,500 \text{ kg}$ (65\,000 lbs).
- (2) *Unknown servo-hydraulic parameters:* These parameters relate to physical response characteristics of the servo-hydraulic system that are not known *a priori*. The leakage coefficient (k_{le}), the table gain factor (k_t) and the servovalve time delay (τ) depend on the internal characteristics of the servovalve-actuator system. The bulk modulus (β) of the actuator fluid/oil can be estimated to approximately 690 MPa (100\,000 psi); however, due to its sensitivity to temperature changes and finite stiffness of the walls of the actuator cylinder, it is very difficult to estimate accurately *a priori* the effective oil bulk modulus.
- (3) *User-set control gain parameters:* The proportional gain (P_{gain}), integral gain (I_{gain}), derivative gain (D_{gain}), feed-forward gain (FF_{gain}) and delta-pressure gain (dP_{gain}) can be set precisely (in digital form) by the operator of the shaking table from the controller front panel to tune the dynamics of the shaking table system.
- (4) *Other parameters:* They consist of the transducers conditioning/conversion constants $K_{x\text{-cond}}$, $K_{D\text{-cond}}$, and $K_{dp\text{-cond}}$, and the dynamic characteristics of the reaction/foundation mass, ω_b and ξ_b , and those of the SDOF payload, ω_p and ξ_p . The conditioning constants were measured to be: $K_{x\text{-cond}} = 0.787 \text{ V/cm}$ (2 V/in), $K_{D\text{-cond}} = K_{x\text{-cond}}/2 = 0.394 \text{ V/cm}$ (1 V/in), and $K_{dp\text{-cond}} = 1/13.05 \text{ V/MPa}$ (1/90 V/ksi). Based on an independent test-analysis correlation study performed by the authors [Trombetti *et al.*, 1997a] encompassing both impulse and forced vibration tests, the following effective SDOF dynamic characteristics were obtained for the foundation/reaction mass: $f_b = \omega_b/2\pi = 27.1 \text{ Hz}$ and $\xi_b = 5.5\%$. The intrinsic dynamic characteristics for the payload(s) used in this test-analysis correlation study will be given on a case-by-case basis in presenting the results.

5.2. Experimental identification of unknown servo-hydraulic parameters

In order to obtain reliable estimates of the unknown servo-hydraulic parameters, k_t , k_{le} , β and τ , a nonlinear least square fit between the experimentally identified

total table transfer function and the analytical model was performed over a wide range of operating and payload conditions. The nonlinear least-square fit consists of minimizingⁱ the Euclidean (or L_2) norm of the difference between the experimental and analytical magnitude transfer functions over the frequency range between 0 and 120 Hz. Due to the extreme jaggedness of the experimentally identified phase transfer function, no attempt was made to least-square fit the experimental and analytical shaking table phase transfer functions. The nonlinear least square fit based on magnitude only of the shaking table transfer function led to successful results in capturing also the salient features of the actual shaking table phase transfer function in accordance with the Bode's gain phase relationship [Bode, 1965; Franklin *et al.*, 1994] stating that for any stable minimum-phase system (i.e. with no RHP zeros or poles), the phase of the system transfer function is uniquely related to the magnitude of the system transfer function.

A large number of least squares fits was performed over a wide range of operating conditions (over 60) of the table (bare and loaded table conditions with various control gain settings). It was observed that, due to the inherently nonlinear nature of servo-hydraulic actuation systems, it was not possible to achieve high-fidelity analytical predictions over a wide range of operating conditions with a unique set of servo-hydraulic parameters (k_t, k_{le}, β, τ). However, the least square optimisation results [Trombetti *et al.*, 1997b] indicate that the servo-hydraulic parameters are sensitive, within engineering accuracy, only to the derivative gain D_{gain} and the effective specimen natural frequency ω_p , while they remain quasi-constant with respect to the other control gains ($P_{\text{gain}}, I_{\text{gain}}, FF_{\text{gain}}, dP_{\text{gain}}$) and the payload weight. Thanks to this limited sensitivity, it was possible to linearise the servo-hydraulic shaking table system about only a few (seven) operating points.^j Thus, the grid of table operating conditions and corresponding sets of identified servo-hydraulic parameters was subdivided into seven groups (or operating points) over which the servo-hydraulic parameters were quasi-constant. The sets of servo-hydraulic parameters characterizing each of these seven groups are given in Tables 1 and 2; they were obtained as rounded-off average of the values of parameters k_t, k_{le}, β , and τ across the group. Table 1 shows the dependence of the effective (optimum) values of the servo-hydraulic parameters upon the value of the derivative control gain, D_{gain} . It is observed that an increase in D_{gain} decreases the value of both the effective table gain factor k_t and the effective oil bulk modulus β , while it increases the value of the effective servovalve time delay τ . On the other hand, the effective leakage coefficient, k_{le} , is found to be independent of the derivative control gain. Table 2 shows the dependence of the effective (optimum) values of the servo-hydraulic parameters

ⁱThe minimization was performed using function "fmins" in *Matlab* [1992] with the tolerance set to 0.01. For more details, the reader is referred to [Trombetti *et al.*, 1997b].

^jThese seven operating points used for effective shaking table system linearisation are: bare table condition for $D_{\text{gain}} = 5, 10, 18$, and 20 ms, respectively, and loaded table condition with $D_{\text{gain}} = 18$ ms and payload fundamental frequency below 50 Hz, between 50 and 100 Hz, and above 100 Hz, respectively.

Table 1. Sets of effective (optimum) servo-hydraulic parameters for bare table condition.

$D_{\text{gain}} = 0$ ms	$D_{\text{gain}} = 10$ ms	$D_{\text{gain}} = 18$ ms	$D_{\text{gain}} = 20$ ms
$k_t = 10.37 \frac{\text{cm}^3}{\text{V s}}$	$k_t = 9.82 \frac{\text{cm}^3}{\text{V s}}$	$k_t = 9.82 \frac{\text{cm}^3}{\text{V s}}$	$k_t = 9.52 \frac{\text{cm}^3}{\text{V s}}$
$\left(k_t = 170 \frac{\text{in}^3}{\text{V s}}\right)$	$\left(k_t = 161 \frac{\text{in}^3}{\text{V s}}\right)$	$\left(k_t = 161 \frac{\text{in}^3}{\text{V s}}\right)$	$\left(k_t = 156 \frac{\text{in}^3}{\text{V s}}\right)$
$\beta = 689.5$ MPa ($\beta = 100\,000$ psi)	$\beta = 586.1$ MPa ($\beta = 85\,000$ psi)	$\beta = 503.3$ MPa ($\beta = 73\,000$ psi)	$\beta = 482.6$ MPa ($\beta = 70\,000$ psi)
$k_{le} = 4.8 \times 10^{-3} \frac{\text{cm}^3}{\text{N s}}$	$k_{le} = 4.8 \times 10^{-3} \frac{\text{cm}^3}{\text{N s}}$	$k_{le} = 4.8 \times 10^{-3} \frac{\text{cm}^3}{\text{N s}}$	$k_{le} = 4.8 \times 10^{-3} \frac{\text{cm}^3}{\text{N s}}$
$\left(k = 1.3 \times 10^{-3} \frac{\text{in}^3}{\text{lbs s}}\right)$	$\left(k_{le} = 1.3 \times 10^{-3} \frac{\text{in}^3}{\text{lbs s}}\right)$	$\left(k_{le} = 1.3 \times 10^{-3} \frac{\text{in}^3}{\text{lbs s}}\right)$	$\left(k_{le} = 1.3 \times 10^{-3} \frac{\text{in}^3}{\text{lbs s}}\right)$
$\tau = 12.0$ ms	$\tau = 13.0$ ms	$\tau = 13.5$ ms	$\tau = 14.0$ ms
Name of parameter set: d0	Name of parameter set: d10	Name of parameter set: d18	Name of parameter set: d20

Table 2. Sets of effective (optimum) servo-hydraulic parameters for loaded table conditions.ⁱ

“Flexible” Payload (fund. freq. < 50 Hz)	“Semi-Rigid” Payload (50 Hz < fund. freq. < 100 Hz)	“Rigid” Payload (fund. freq. > 100 Hz)
$k_t = 9.15 \frac{\text{cm}^3}{\text{V s}}$	$k_t = 11.81 \frac{\text{cm}^3}{\text{V s}}$	$k_t = 11.29 \frac{\text{cm}^3}{\text{V s}}$
$\left(k_t = 150 \frac{\text{cm}^3}{\text{V s}}\right)$	$\left(k_t = 193.5 \frac{\text{cm}^3}{\text{V s}}\right)$	$\left(k_t = 185 \frac{\text{cm}^3}{\text{V s}}\right)$
$\beta = 427.5 \text{ MPa}$ $(\beta = 62\,000 \text{ psi})$	$\beta = 510.2 \text{ MPa}$ $(\beta = 74\,000 \text{ psi})$	$\beta = 524.0 \text{ MPa}$ $(\beta = 76\,000 \text{ psi})$
$k_{le} = 4.8 \times 10^{-3} \frac{\text{cm}^3}{\text{N s}}$	$k_{le} = 7.0 \times 10^{-3} \frac{\text{cm}^3}{\text{N s}}$	$k_{le} = 4.8 \times 10^{-3} \frac{\text{cm}^3}{\text{N s}}$
$\left(k_{le} = 1.3 \times 10^{-3} \frac{\text{in}^3}{\text{lbs s}}\right)$	$\left(k_{le} = 1.9 \times 10^{-3} \frac{\text{in}^3}{\text{lbs s}}\right)$	$\left(k_{le} = 1.3 \times 10^{-3} \frac{\text{in}^3}{\text{lbs s}}\right)$
$\tau = 14.0 \text{ ms}$	$\tau = 10.3 \text{ ms}$	$\tau = 10.42 \text{ ms}$
name of parameter set: pf	name of parameter set: pfr	name of parameter set: pr

ⁱThese optimum servovalve parameters were obtained under the “optimum” control gain setting for bare table condition.

upon the flexibility of the test specimen as measured by its fundamental natural frequency. It is not possible to identify a clear trend in the variation of these effective parameters for increasing payload fundamental frequency, thus suggesting that these parameters are affected by the dynamic interaction between the test specimen and oil column in the actuator.

For each of the numerous operating conditions considered, the use of the servo-hydraulic parameters of the appropriate operating point enables a good to very good correlation between experimental and analytical results as shown later in the paper. Therefore, the servo-hydraulic parameters given in Tables 1 and 2 of the paper should be interpreted as effective parameters aggregating the effects of various physical phenomena in the controller, servovalve, and actuator.

6. Analytical and Experimental Table Sensitivity to Control Gain Parameters

This section presents results on shaking table transfer function sensitivities to user-set control gain parameters (P_{gain} , I_{gain} , D_{gain} , FF_{gain} and dP_{gain}) in the context of a test-analysis comparison study. These sensitivity results were obtained for bare table condition and, in order to enhance the individual effects of the various control gain parameters, using control gain settings that are different from those used for optimum shaking table performance as defined later in Sec. 7. The shaking table transfer function sensitivity to control gain parameters was obtained by increasing,

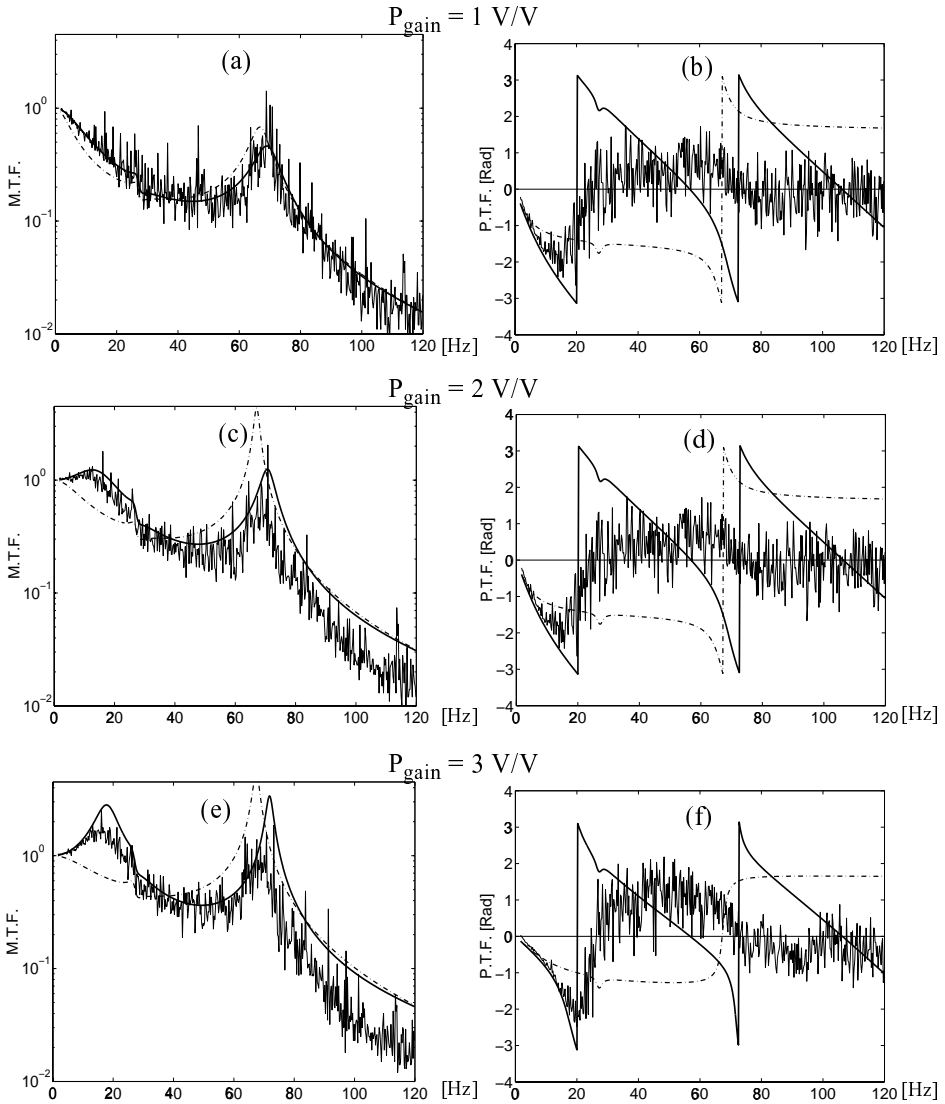


Fig. 3. Total shaking table transfer function for $P_{\text{gain}} = 1, 2, 3 \text{ V/V}$, $I_{\text{gain}} = D_{\text{gain}} = FF_{\text{gain}} = dP_{\text{gain}} = 0$ (thick solid line = analytical T.F. with non-zero servo valve time delay τ , dashed-dot line = analytical T.F. with zero servo valve time delay ($\tau = 0$), thin solid line = experimentally identified T.F.).

starting from zero, the value of one control gain parameter, while keeping the other control gains at zero.^k

^kExcept for the proportional gain P_{gain} that was kept at 1 V/V as a zero value of P_{gain} leads to a degenerated, unacceptable performance of the shaking table.

6.1. Proportional gain (P_{gain})

6.1.1. Magnitude of the total shaking table transfer function (M.T.F.)

Figures 3(a), (c) and (e) show the magnitude of the shaking table transfer function (M.T.F.) for values of the P_{gain} increasing from 1.0 to 3.0 V/V.¹ Notice the large peak in the transfer function at approximately 70 Hz. This is the oil column peak that is due to the resonance behavior of the SDOF system having as spring the oil column enclosed in the two actuator chambers and as mass that of the table platform, m_t , including actuator piston/arm and swivel head. The oil column frequency is given by [Conte and Trombetti, 2000]

$$f_{\text{oil}} = (A/\pi)\sqrt{\beta/(Vm_t)} \quad (11)$$

and acts here essentially as an upper cut-off frequency of the shaking table dynamics. The distortion in the shaking table M.T.F. (both experimental and analytical) at a frequency of about 27 Hz is due to the flexibility of the foundation/reaction mass (i.e. resonance frequency of reaction mass). An increase in the P_{gain} raises the magnitude of the table transfer function over the whole frequency bandwidth of the system. This increase in the M.T.F. is particularly pronounced around 15 Hz where a new spectral peak originates and at the oil column frequency around 70 Hz. Notice that the analytical predictions incorporating the servovalve time delay τ (thick solid line) are in close agreement with the experimental results (thin solid line).^m In contrast, the analytical predictions assuming a zero servovalve time delay (dashed-dot line) are able to capture only the overall change of the shaking table M.T.F. for increasing P_{gain} . Notice that the analytical model with $\tau = 0$ does not capture the arising spectral peak centered at about 15 Hz due to increasing P_{gain} , and considerably overestimates the size of the oil column peak for $P_{\text{gain}} = 2.0$ V/V as shown in Figs. 3(c) and (e).

6.1.2. Phase of the total shaking table transfer function (P.T.F.)

Figures 3(b), (d) and (f) display the phase of the total shaking table transfer function (P.T.F.) for the proportional gain (P_{gain}) increasing from 1.0 to 3.0 V/V. The main effect of increasing P_{gain} is a change in the curvature (from upward to downward) of the P.T.F. in the frequency range from 0 to 20 Hz. The notch at about 27 Hz visible in the analytical P.T.F. reflects the resonance frequency of the foundation/reaction mass.

¹All other control gains were set to zero. The set of servo-hydraulic parameters used in the analytical model for all values of P_{gain} is the one referred to as “d0” in Table 1. The good correlation obtained between analytical and experimental results confirms that the servo-hydraulic parameters are independent of the proportional gain.

^mThe jaggedness characterising the experimentally identified shaking table M.T.F. is inherent to and consistent with the statistical uncertainties of the wide band spectral estimation method adopted herein and is also due to electrical line noise [Trombetti *et al.*, 1997b].

As for the magnitude transfer function, the analytical model incorporating the servovalve time delay matches significantly better the experimentally identified P.T.F. than the analytical model with zero servovalve time delay, especially in the low to intermediate frequency range from 0 to 20 Hz. Due to the averaging process used in the Bartlett's procedure, the inherent statistical uncertainty of the estimated shaking table transfer function, and the conventional calculation/representation of the phase angle between $-\pi$ and $+\pi$, the actual shaking table phase transfer function in the neighborhood of $-\pi$ and $+\pi$ is incorrectly estimated as close to zero. For example, two window estimates of $-(\pi - d\phi)$ and $+(\pi - d\phi)$ of an actual phase value of π average out to zero.

The above results already show that the inclusion of a servovalve time delay in the analytical model of the shaking table system is crucial to achieve a good correlation between experimental and analytical results. This is further confirmed by the test-analysis comparison results shown in the next sections. Therefore, for the sake of conciseness, the analytical prediction of the shaking table transfer function with zero servovalve time delay will be presented graphically for each case considered, but without any further comment on the inadequate modelling obtained by neglecting the servovalve time delay.

6.2. Integral gain (I_{gain})

6.2.1. Magnitude of the total shaking table transfer function (M.T.F.)

Figures 4(a), (c) and (e) plot the magnitude of the shaking table transfer function (M.T.F.) for the integral gain (I_{gain}) increasing from 0 to 40 Hz.^a Both experimental and analytical results show a significant increase in the M.T.F. in the very low frequency range (0–10 Hz) and the rise of a narrow spectral peak centered at about 6 Hz. It is noteworthy that the I_{gain} does not affect at all the shaking table transfer function above 20 Hz. For integral gains of 0, 20 and 40 Hz, the analytical model incorporating a servovalve time delay τ is found to be in very good agreement with the experimental results. It captures accurately both in amplitude and frequency all the salient features (e.g. peak and notch effect due to base flexibility, oil column peak) of the experimentally derived M.T.F.

6.2.2. Phase of the total shaking table transfer function (P.T.F.)

Figures 4(b), (d) and (f) display the phase of the total shaking table transfer function (P.T.F.) for increasing values of the integral control gain, I_{gain} , from 0 to 40 Hz. The only appreciable effect of increasing I_{gain} is an increase (“steepening”) of the phase lag in the low frequency range from 0 to 20 Hz.

The analytical model with servovalve time delay τ predicts very well the experimentally identified P.T.F. in the low frequency range from 0 to 20 Hz, especially in the case of $I_{\text{gain}} = 40$ Hz shown in Fig. 4(f).

^aThe P_{gain} was set to 1.0 (V/V) and all other control gains were set to zero. The set of servohydraulic parameters used in the analytical models is the one referred to as “d0” in Table 1.

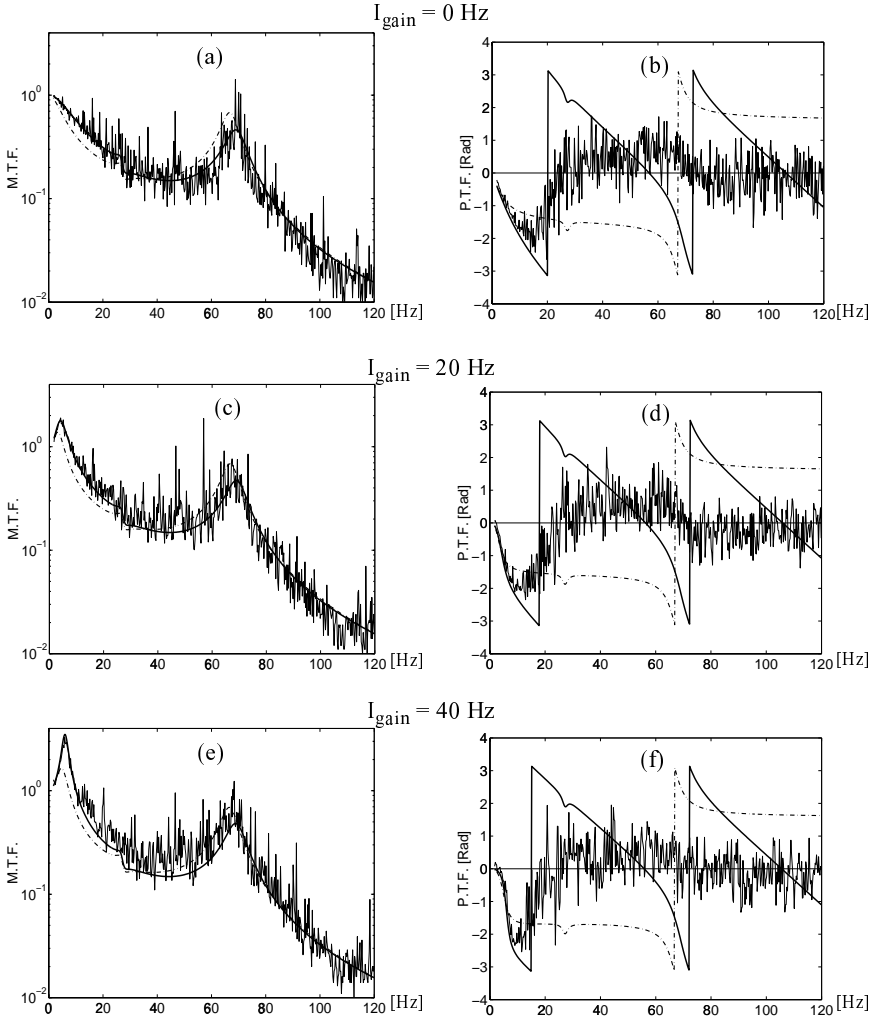


Fig. 4. Total shaking table transfer function for $I_{\text{gain}} = 0, 20, 40$ Hz, $P_{\text{gain}} = 1$ V/V, $D_{\text{gain}} = FF_{\text{gain}} = dP_{\text{gain}} = 0$ (thick solid line = analytical T.F. with non-zero servo valve time delay τ , dashed-dot line = analytical T.F. with zero servo valve time delay ($\tau = 0$), thin solid line = experimentally identified T.F.).

6.3. Derivative gain (D_{gain})

6.3.1. Magnitude of the total shaking table transfer function (M.T.F.)

Figures 5(a), (c) and (e) show the M.T.F. for values of the derivative control gain, D_{gain} , increasing from 0 to 20 ms.^o An increase in this control gain raises the M.T.F.

^oThe P_{gain} was set to 1.0 V/V and all other control gains were set to zero. The set of servo-hydraulic parameters used in the analytical models depends on the value of the derivative gain, D_{gain} , as given in Table 1.

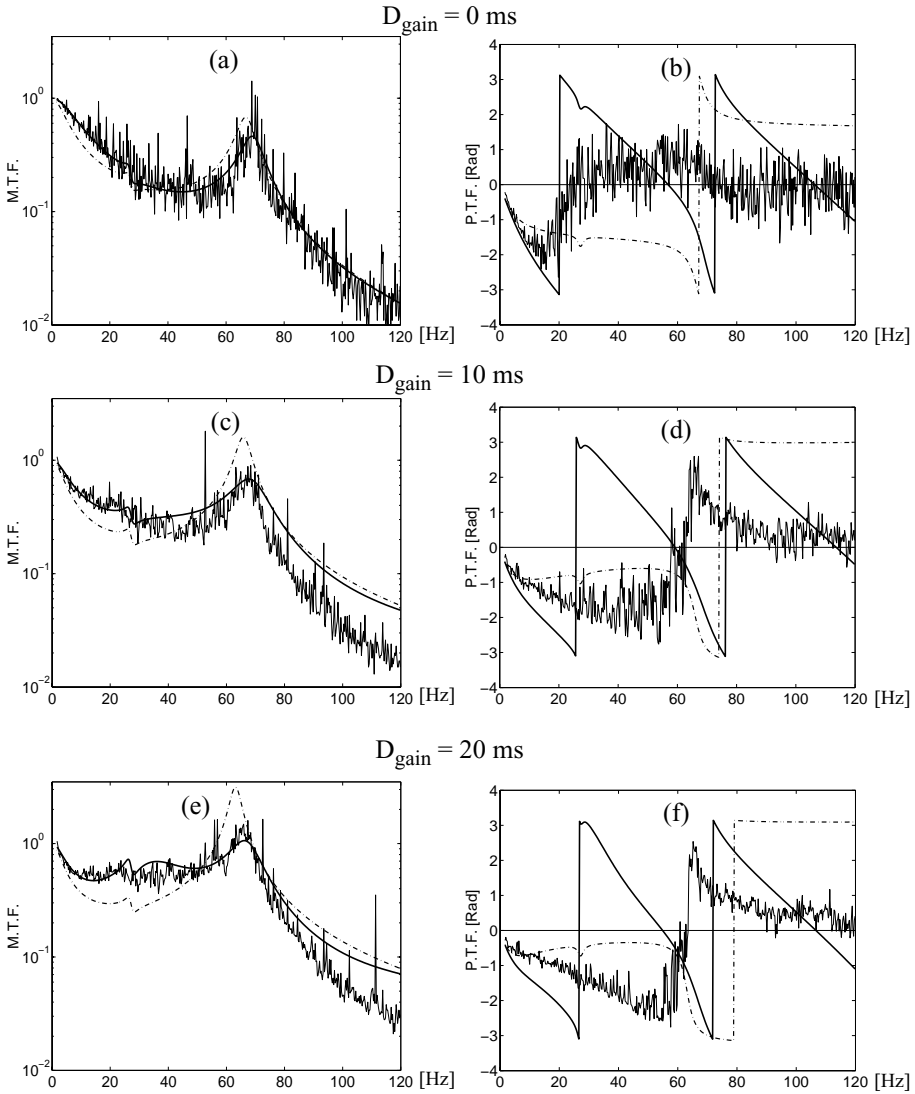


Fig. 5. Total shaking table transfer function for $D_{\text{gain}} = 0, 10, 20$ ms, $P_{\text{gain}} = 1$ V/V, $I_{\text{gain}} = FF_{\text{gain}} = dP_{\text{gain}} = 0$ (thick solid line = analytical T.F. with non-zero servovalve time delay τ , dashed-dot line = analytical T.F. with zero servovalve time delay ($\tau = 0$), thin solid line = experimentally identified T.F.).

in the intermediate frequency range (from 10 to 60 Hz) and lowers the oil column frequency from approximately 70 Hz to 65 Hz. Notice the peak and notch effect at 27 Hz due to foundation compliance.

The analytical model accounting for the servovalve time delay τ (as given in Table 1) is found to be in excellent agreement with the experimentally identified M.T.F.

6.3.2. *Phase of the total shaking table transfer function (P.T.F.)*

Figures 5(b), (d) and (f) depict the phase of the total shaking table transfer function (P.T.F.) for D_{gain} increasing from 0 to 20 ms. It is observed that an increase in D_{gain} improves (i.e. lowers) significantly (by about three-fold) the actual phase lag of the table in the low frequency range from 0 to 20 Hz. Notice that most of the

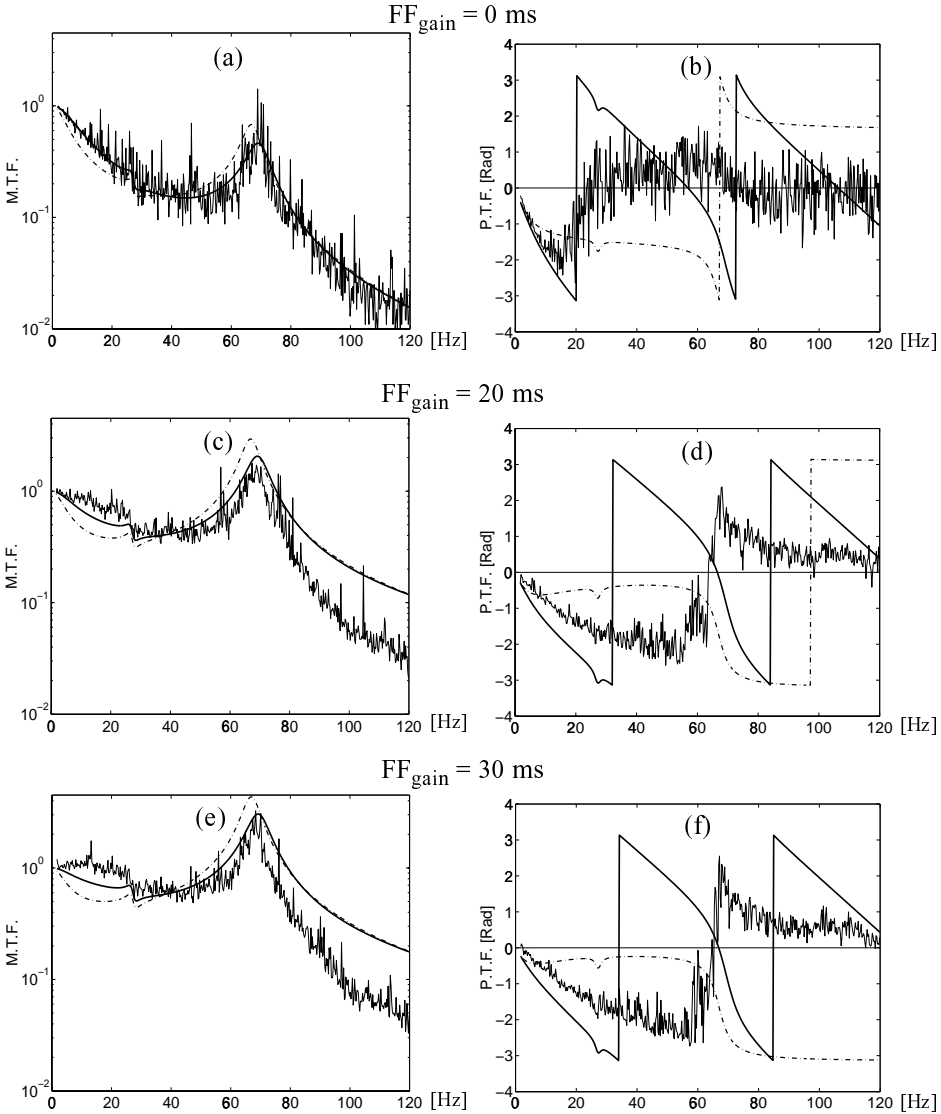


Fig. 6. Total shaking table transfer function for $FF_{\text{gain}} = 0, 20, 30$ ms, $P_{\text{gain}} = 1$ V/V, $I_{\text{gain}} = D_{\text{gain}} = dP_{\text{gain}} = 0$ (thick solid line = analytical T.F. with non-zero servovalve time delay τ , dashed-dot line = analytical T.F. with zero servovalve time delay ($\tau = 0$), thin solid line = experimentally identified T.F.).

reduction in the phase transfer function occurs as D_{gain} increases from 0 to 10 ms. Further increase in D_{gain} has practically no effect on the P.T.F.

In this case, the analytical model prediction of the P.T.F. accounting for servovalve time delay does not capture accurately, as compared to other cases, the experimentally identified P.T.F. The latter is found to lie between the analytical predictions with zero and non-zero servovalve time delay in the low frequency range between 0 and 20 Hz.

6.4. Feed-forward gain (FF_{gain})

6.4.1. Magnitude of the total shaking table transfer function (M.T.F.)

Figures 6(a), (c) and (e) present the magnitude of the total shaking table transfer function (M.T.F.) for FF_{gain} increasing from 0 to 30 ms.^P This increase in the FF_{gain} raises (by about three-fold) the magnitude of the total shaking table transfer function almost uniformly over the entire frequency bandwidth of the shaking table system, thus maintaining the shape of the M.T.F.

The analytical model that incorporates the servovalve time delay τ is in good agreement with the experimentally identified M.T.F.

6.4.2. Phase of the total shaking table transfer function (P.T.F.)

Figures 6(b), (d) and (f) show the phase of the total shaking table transfer function (P.T.F.) for value of the FF_{gain} increasing from 0 to 30 ms. It is found that such an increase in the FF_{gain} reduces significantly the phase lag of the table in the low frequency range and further increase in the FF_{gain} has practically no effect on the table P.T.F. The experimentally identified shaking table P.T.F. in the low frequency range lies between the analytical predictions with zero and non-zero servovalve time delay, respectively.

It is worth noting that the D_{gain} and FF_{gain} , both associated with the differential operator in the control algorithm, have very similar effects upon the total shaking table phase transfer function.

6.5. Differential-pressure gain (dP_{gain})

6.5.1. Magnitude of the total shaking table transfer function (M.T.F.)

Figures 7(a), (c) and (e) are plots of the magnitude of the total shaking table transfer function (M.T.F.) for the differential-pressure gain, dP_{gain} , increasing from 0. to 3.0 V/V.^q It is observed that the main effects of increasing the dP_{gain} are: (1) a significant reduction (about three-fold for $dP_{\text{gain}} = 3.0$ V/V) of the amplitude of

^PThe P_{gain} was set to 1.0 (V/V) and all other control gains were set to zero. The set of servo-hydraulic parameters used in the analytical models is the one referred to as “d0” in Table 1.

^qThe P_{gain} was set to 1.0 V/V and all other control gains were set to zero. The set of servo-hydraulic parameters used in the analytical models is the one referred to as “d0” in Table 1.

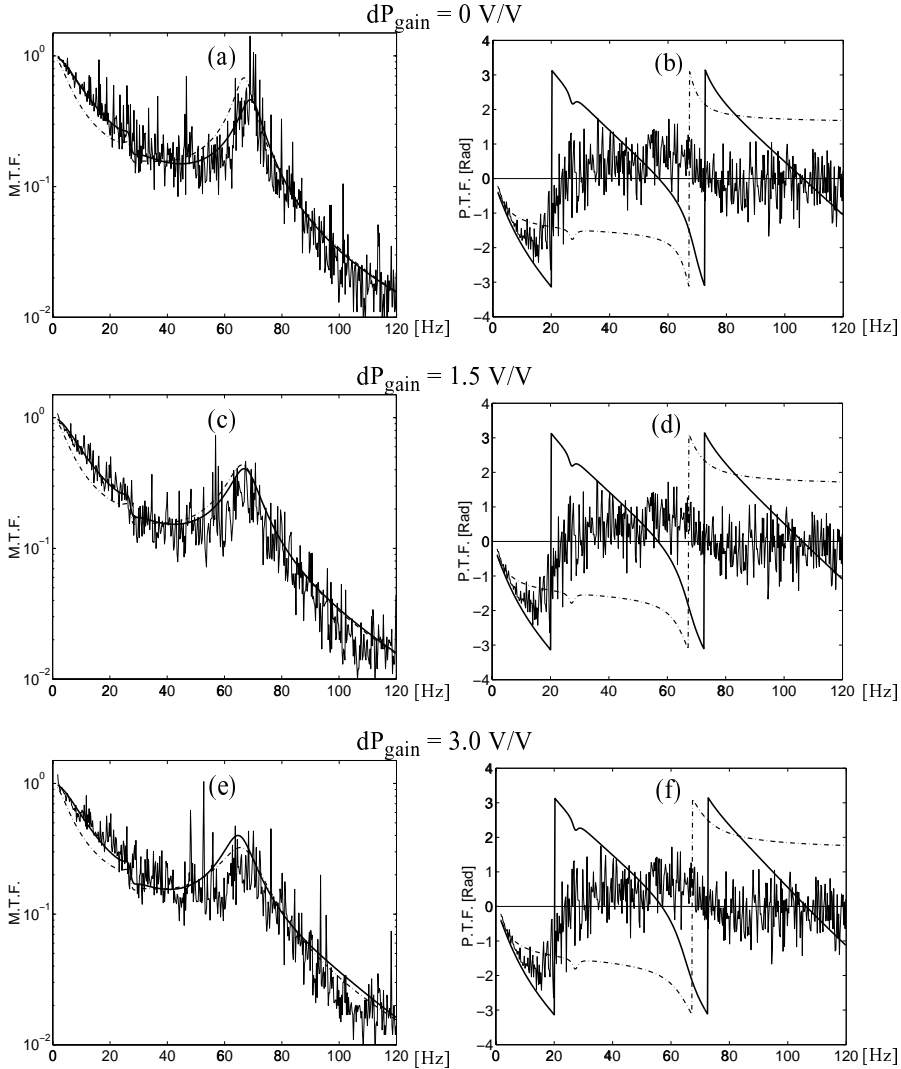


Fig. 7. Total shaking table transfer function for $dP_{\text{gain}} = 0, 1.5, 3.0 \text{ V/V}$, $P_{\text{gain}} = 1 \text{ V/V}$, $I_{\text{gain}} = D_{\text{gain}} = FF_{\text{gain}} = 0$ (thick solid line = analytical T.F. with non-zero servo valve time delay τ , dashed-dot line = analytical T.F. with zero servo valve time delay ($\tau = 0$), thin solid line = experimentally identified T.F.).

the oil column peak (thus justifying the common reference to dP_{gain} as “numerical” damping) and (2) a lowering of the oil column frequency of about 5 Hz. The dP_{gain} is therefore useful to compensate for the amplification of the oil column peak caused by increasing the proportional, the derivative, or the feedback gain.

The analytical model that incorporates the servo valve time delay τ agrees very well with the experimentally identified M.T.F., except for some overestimation in the spectral region around the oil column frequency. Here, the difference between the

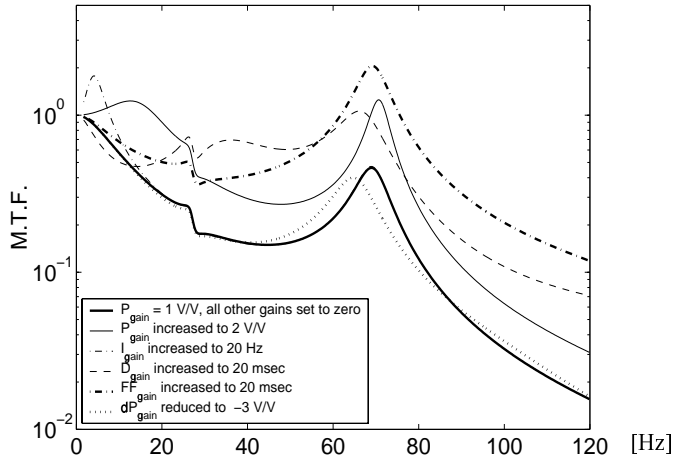


Fig. 8. Sensitivity of analytical total shaking table transfer function to control gain parameters for bare table condition.

analytical predictions obtained with zero and non-zero servovalve time delay, respectively, is smaller than in the previous cases considered (Figs. 3–6), with nonetheless a more accurate prediction achieved by incorporating the servovalve time delay.

6.5.2. Phase of the total shaking table transfer function (P.T.F.)

Figures 7(b), (d) and (f) provide plots of the phase of the total shaking table transfer function (P.T.F.) as the dP_{gain} increases from 0. to 3.0 V/V. From these plots, it is observed that an increase in the dP_{gain} has insignificant effects on the table P.T.F. The experimentally identified P.T.F. lies between the analytical predictions with zero and non-zero servovalve time delay, respectively, with slightly better prediction by the analytical model with non-zero servovalve time delay.

In summary, the results presented in this section show that the analytical model that incorporates the servovalve time delay^r has a very good predictive capability (qualitative and quantitative) over a wide range of control gain setting and payload conditions. In contrast, the analytical model with zero servovalve time delay is able to provide only an overall qualitative prediction of the total shaking table transfer function. The above test-analysis correlation and parametric sensitivity studies shed light into the effects (absolute and relative) that the five control gain parameters have upon the total shaking table transfer function in the various spectral regions. The total shaking table transfer function can be considerably modified both in shape and absolute value via the control gain parameters as synthesized in Fig. 8.

^rAlthough widely used in control theory, the time delay has not been used for previous analytical modelling of shaking table systems and servo-hydraulic actuators [Rea *et al.*, 1977; Hwang *et al.*, 1987; Rinawi and Clough, 1991; Dyke *et al.*, 1995], therefore making it a unique feature of the analytical shaking table model developed by the authors [Conte and Trombetti, 2000].

Next sections show how the control gain parameters are used jointly to optimize the dynamic performance of the shaking table system for bare (Sec. 7) and loaded (Sec. 8.4) table conditions.

7. Experimental and Analytical Dynamic Performance of the Shaking Table under the “Optimal” Control Gain Setting

Based on the results of the sensitivity analysis to control gain parameters presented in the previous section, a search for the optimal gain setting under bare table condition was performed. The objective of this optimisation problem was to minimise, under the physical constraint of the shaking table coupled dynamics, both the root-mean-square and the maximum absolute value of the departure from unity (= ideal total shaking table transfer function) of the magnitude of the total shaking table transfer function over the frequency range between 0 and 120 Hz. Guided by the sensitivities to control gains of the total shaking table transfer function provided by the high-fidelity analytical model accounting for servovalve time delay, the optimum search was conducted by physically varying the user-set control gains, experimentally identifying the shaking table transfer function, and evaluating the objective/error functions [Trombetti *et al.*, 1997b]. This optimisation/tuning process led to the “optimum” control gain setting given in Table 3.

Table 3. “Optimal” control gain setting for bare table condition.

$P_{\text{gain}} = 1.8 \text{ V/V}$	$FF_{\text{gain}} = 18.0 \text{ ms}$
$I_{\text{gain}} = 40.0 \text{ Hz}$	$dP_{\text{gain}} = -3.0 \text{ V/V}$
$D_{\text{gain}} = 18.0 \text{ ms}$	

7.1. Magnitude of the total shaking table transfer function (M.T.F.)

Figure 9(a) displays the magnitude of the experimentally identified and analytically predicted total shaking table transfer functions under the “optimal” control gain setting for bare table condition.⁵ Observe that, due to the physical constraint of the shaking table system dynamics, an ideal transfer function of unity cannot be achieved. Nevertheless, the optimum actual shaking table M.T.F. obtained oscillates around unity over the frequency range between 0 and 120 Hz. Notice the unavoidable peaks at approximately 5 Hz (induced by the relatively high optimum value of I_{gain}) and 67 Hz (oil column peak), and the peak and notch effect at about 27 Hz (due to foundation/reaction mass resonance).

⁵The set of servo-hydraulic parameters used in the analytical models is the one referred to as “d18” in Table 1, as a value of $D_{\text{gain}} = 18 \text{ ms}$ was obtained for the optimum derivative control gain.

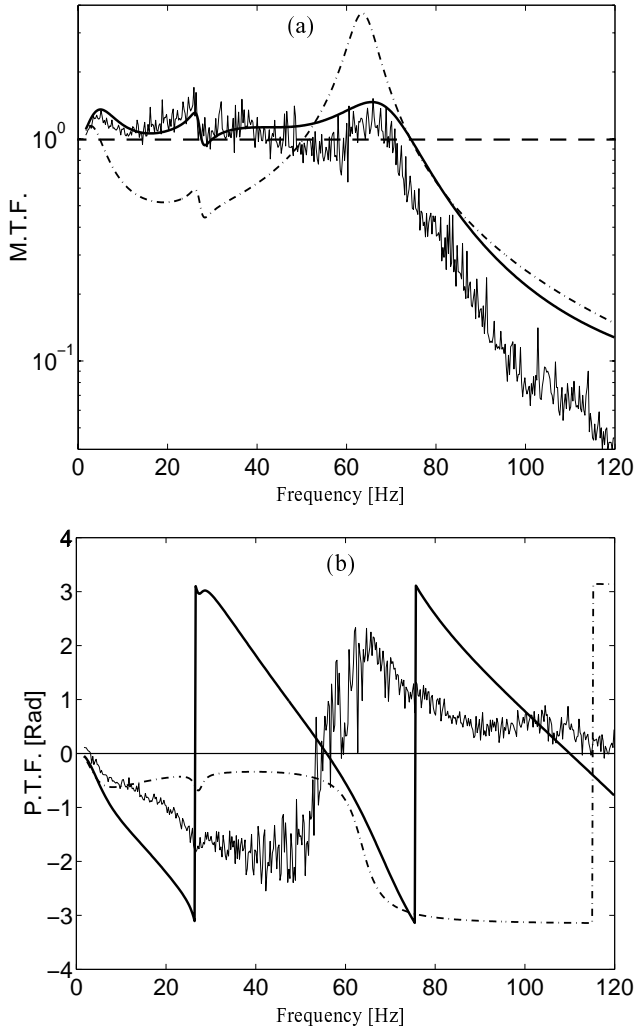


Fig. 9. (a) Magnitude and (b) phase of the total shaking table transfer function for the “optimum” control gain setting under bare table condition (*thick solid line = analytical T.F. with non-zero servovalve time delay τ , dashed-dot line = analytical T.F. with zero servovalve time delay ($\tau = 0$), thin solid line = experimentally identified T.F.*)

The analytical model incorporating the servovalve time delay τ matches very well the experimentally identified total shaking table M.T.F., capturing all the peaks and notches displayed by the experimentally derived M.T.F., with some overestimation of the magnitude of the oil column peak.

7.2. Phase of the total shaking table transfer function (P.T.F.)

The phases (P.T.F) of the experimentally identified and analytically predicted total shaking table transfer functions are shown in Fig. 9(b). The experimentally

derived P.T.F. lies between the two analytical predictions (with zero and non-zero servovalve time delay, respectively) in the low frequency range, with however a better prediction by the model accounting for non-zero servovalve time delay.

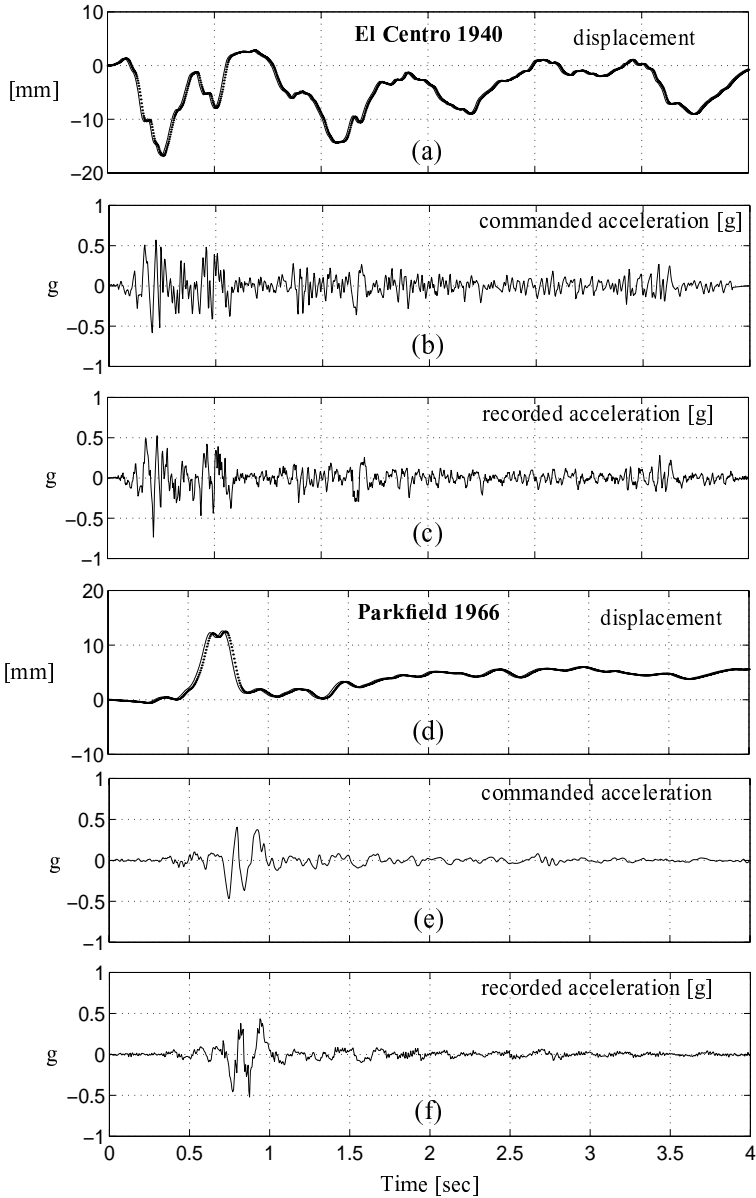


Fig. 10. Displacement and acceleration time history reproduction for (a), (b), (c): El Centro 1940 Earthquake record (N-S comp.) and (d), (e), (f): Parkfield 1966 Earthquake record (bare table condition, “optimum” control gain setting for bare table condition) (solid line = commanded/target displacement, dotted line = recorded displacement).

7.3. Time history reproduction capability of the shaking table

The capabilities of the optimally tuned bare shaking table in reproducing earthquake displacement and acceleration records are shown in Fig. 10. Figures 10(a), (b) and (c) correspond to the well known 1940 El Centro Earthquake record (N-S component), while Figs. 10(d), (e) and (f) correspond to the 1966 Parkfield Earthquake record. These two records are scaled both in time and amplitude for similitude requirements and sub-incremented at a sampling rate of 4000 Hz. The commanded and achieved ground/table displacement histories are shown in Figs. 10(a) and (d) for El Centro 1940 and Parkfield 1966, respectively. The corresponding target and achieved table acceleration time histories are plotted in Figs. 10(b) and (c), respectively, for El Centro 1940, and in Figs. 10(e) and (f), respectively, for Parkfield 1966. It is observed that a high degree of fidelity is achieved in both displacement and acceleration time history reproduction, with however a lesser degree of accuracy for acceleration than for displacement, which is expected since the earthquake simulator is stroke/displacement controlled.

8. Experimental and Analytical Shaking Table Transfer Function Sensitivities to Payload Characteristics

This section presents the results of a correlation study between the experimentally identified and analytically predicted shaking table sensitivities to a selected set of both “rigid” and flexible payloads. The objectives of this section are: (1) to investigate whether and how the actual total shaking table transfer function is affected by large (relative to the table capacity) “rigid” and flexible payloads, and (2) to determine the predictive capabilities of the analytical shaking table model for loaded table conditions.

For this purpose, the Rice University shaking table was loaded with: (1) a series of “rigid” payloads each consisting of a number of 68 kg (150 lbs) concrete blocks clamped to the table platform through 11 mm (7/16 in) bolts, and (2) a flexible payload consisting of a reduced scale three-storey one bay by one bay steel moment resisting building frame.^t

The user-set table control gain parameters used to obtain the results presented in this section correspond to the optimal gain setting for bare table condition described in the previous section,^u except for a reduction of I_{gain} from 40 Hz to 30 Hz and zeroing of dP_{gain} . It is worth pointing out that in the present sensitivity analysis, payloads ranging from 68 to 408 kg (150 to 900 lbs) are considered, thus reaching 60 percent of the table design maximum payload capacity of 700 kg (1500 lbs).

^tFor more details about these payload conditions, the interested reader is referred to the original reports by Trombetti *et al.* [1997 (Appendix B)].

^uThe optimal control gain setting for the loaded shaking table differs from that for bare table condition. The optimal gain setting for bare table condition was used to enhance the effects of the payloads on the shaking table transfer function. The issue of re-tuning the control gain parameters for loaded table condition is addressed in Sec. 9 of this paper.

8.1. “Rigid” payload (with perfectly rigid modelling)

Figures 11(a) through (f) show the comparison between the experimentally identified and analytically predicted total shaking table transfer functions for 68, 204, and 408 kg (150, 450, and 900 lbs) “rigid” payloads made of concrete blocks clamped to the table platform. These payloads were analytically modeled as infinitely stiff (i.e. rigid) and, therefore, their mass was simply added to that of the table platform.^v

8.1.1. Magnitude of the total shaking table transfer function (M.T.F.)

Figures 11(a), (c) and (e) display the magnitude of the total shaking table transfer function (M.T.F.) for increasing “rigid” payload weight. These figures indicate that the presence on the table of a “rigid” payload of increasing weight reduces the bandwidth of the shaking table system and raises the M.T.F. within the system bandwidth, producing a wide spectral peak (centered between 36 and 40 Hz depending on the payload weight) referred to hereafter as “central” peak. The largest relative increase in the M.T.F. at the location of the central peak occurs with the addition of the 68 kg (150 lbs) “rigid” payload for which the experimental M.T.F. increases from approximately 1.2 for bare table condition, see Fig. 9(a), to about 2.7, see Fig. 11(a). The addition of heavier “rigid” payloads does not increase proportionally the amplitude of the newly formed “central” peak: the height of the experimental “central” peak grows from about 2.7 for the 68 kg (150 lbs) payload to about 3.5 for the 204 kg (450 lbs) payload and to about 5.3 for the 408 kg (900 lbs) payload. Careful examination of the magnitude of the experimental transfer function indicates that the central peak does not correspond to the shifted oil column peak (as predicted by the oil column frequency in Eq. (11) as another (smaller) spectral peak is present in the experimentally derived transfer function at about 57 Hz. As shown in the next section, this smaller experimental spectral peak can be predicted by the analytical shaking table model provided that the actual finite stiffness of the here assumed perfectly rigid payload clamping system is taken into account. It is also observed that the peak at about 27 Hz due to foundation/reaction mass compliance is amplified by the presence of a “rigid” payload on the table. Its amplitude grows from about 1.5 for bare table condition, see Fig. 9(a), to about 1.7, 2.0, and 3.0 for a “rigid” payload of 68, 204, and 408 kg (150, 450, and 900 lbs), respectively.

The analytical model incorporating the servovalve time delay τ is found to be in very good agreement with the experimental results for all “rigid” payloads considered here, even though the corresponding analytical prediction does not capture

^vThe set of servo-hydraulic parameters used in the analytical model is the one referred to as “pr” in Table 2. As explained in Sec. 5, this set provides the least square fit between analytical and experimental transfer functions of the table loaded with very stiff (“rigid”) payload (i.e. characterised by natural frequencies above 100 Hz).

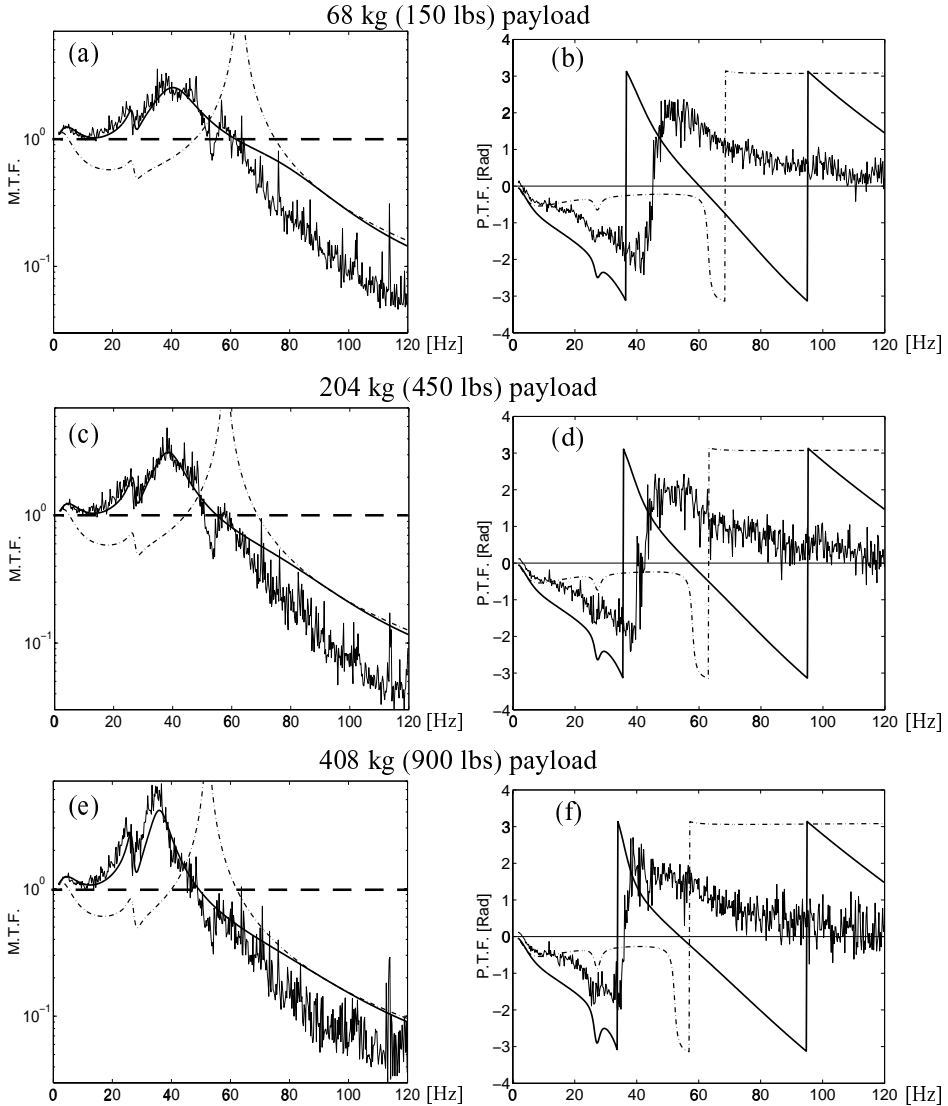


Fig. 11. Total shaking table transfer function for “rigid” payloads of 68, 204, and 408 kg (150, 450, and 900 lbs) with infinitely stiff analytical modelling (*thick solid line = analytical T.F. with non-zero servo valve time delay τ , dashed dot line = analytical T.F. with zero servo valve time delay ($\tau = 0$), thin solid line = experimentally identified T.F.*).

the above mentioned small spectral peak located at about 57 Hz. In spite of using a single set (“**pr**”) of servo-hydraulic parameters, notice the level of detail with which the analytical model is able to capture (1) the characteristics of the experimentally derived M.T.F. and (2) their variations due to “rigid” payload of increasing weight (i.e. amplitude of spectral peaks at about 5 and 27 Hz, and amplitude, frequency shift, and narrowing of “central” peak).

8.1.2. *Phase of the total shaking table transfer function (P.T.F.)*

Figures 11(b), (d) and (f) show the phase of the total shaking table transfer function for “rigid” payloads of 68, 204, and 408 kg (150, 450, and 900 lbs), respectively. From these plots, it is observed that a “rigid” payload of increasing weight distorts increasingly the shape of the experimentally identified P.T.F. in the spectral region around the resonant frequency (~ 27 Hz) of the foundation/reaction mass. It is found that the experimentally identified P.T.F. lies between the analytical predictions with zero and non-zero servovalve time delay, respectively, in the frequency range between 0 and 40 Hz.

8.2. *“Rigid” payload (with partially flexible modelling)*

As in the previous section, this section deals with the comparison between experimentally identified and analytically predicted total shaking table transfer functions for “rigid” payload conditions. Here, however, we use an improved analytical model of the shaking table transfer function which accounts for the actual finite stiffness of the system employed to clamp the concrete blocks to the table platform. In this analytical model of the shaking table system with partially flexible modelling of the “rigid” payload, the latter is modeled as the combination of an SDOF payload with a natural frequency of 52 Hz (obtained analytically by using the bending stiffness of the clamping bolts) and a perfectly rigidly clamped payload.^w The set of servo-hydraulic parameters used in the analytical model is the one referred to as “**pfir**” in Table 2.^x

8.2.1. *Magnitude of the total shaking table transfer function (M.T.F.)*

Figures 12(a), (c) and (e) compare the experimentally identified and analytically predicted (using partially flexible modelling of the payload) magnitude of the total shaking table transfer function (M.T.F.) for “rigid” payloads of 68, 204, and 408 kg (150, 450, and 900 lbs). Notice that the improved analytical model incorporating servovalve time delay captures very well the experimentally identified spectral peaks at approximately 5 Hz and 27 Hz, and the “central” peak, which was also the case for the analytical model with assumed perfectly rigid payload. A unique feature of this improved analytical model is that it is moreover able to capture very well and explain the small spectral peak identified experimentally at about 57 Hz. A previous analytical study performed by the authors [Trombetti *et al.*, 1997a; Conte and Trombetti, 2000] in fact reveals that, in the presence of an SDOF payload characterised by a natural frequency close to the oil column frequency (for bare table condition), the oil column peak splits into two spectral peaks.

^wFor the rationale behind this equivalent dynamic modelling of the “rigid” payload, the interested reader is referred to the original report by the authors [Trombetti *et al.*, 1997a].

^xThis set of servo-hydraulic parameters is used because, as explained in Sec. 5, it is the one which provides a least-square fit between analytical and experimental shaking table transfer functions for payloads with a natural (fundamental) frequency between 50 and 100 Hz.

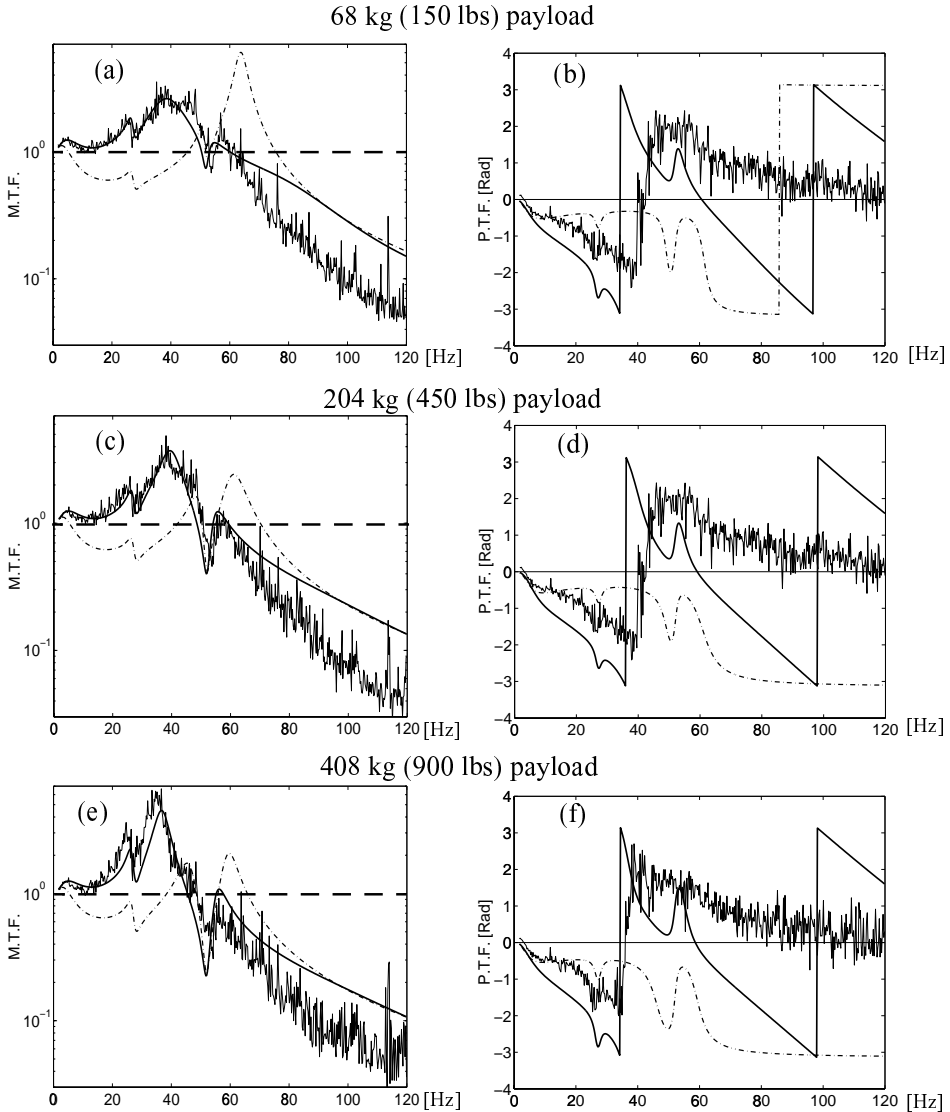


Fig. 12. Total shaking table transfer function for “rigid” payloads of 68, 204, and 408 kg (150, 450, and 900 lbs) with partially flexible analytical modelling (*thick solid line = analytical T.F. with non-zero servo valve time delay τ , dashed dot line = analytical T.F. with zero servo valve time delay ($\tau = 0$), thin solid line = experimentally identified T.F.*).

In accordance with this analytical prediction, the shaking table M.T.F. identified experimentally for 68, 204, and 408 kg (150, 450, and 900 lbs) “rigid” payloads displays these two peaks, one of larger amplitude centered at a frequency between 36 and 42 Hz depending on the payload weight and the other at about 57 Hz. The very good agreement obtained here between the experimental and analytical (incorporating the servo valve time delay) M.T.F.’s suggests that the so-called

“rigid” payloads effectively behave as flexible SDOF payloads with high natural frequency.

The above is a perfect illustration on how the joint use of analytical modelling and prediction (from a physics-based well calibrated analytical model) and experimental analysis can lead to the correct physical interpretations of shaking table test results.

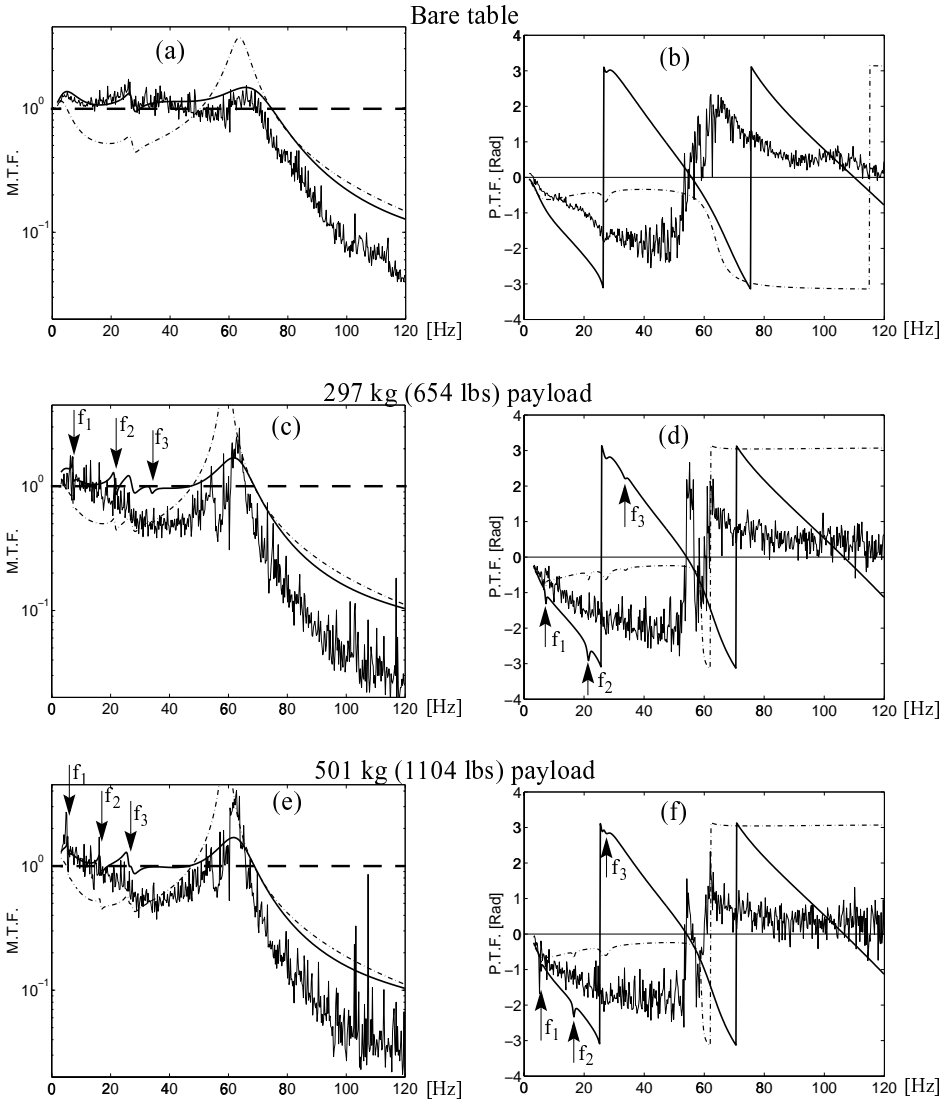


Fig. 13. Total shaking table transfer function for bare table condition and shaking table loaded with 297 and 501 kg (654 and 1104 lbs) flexible payloads (*thick solid line = analytical M.T.F. with non-zero servo valve time delay τ , dashed dot line = analytical M.T.F. with zero servo valve time delay ($\tau = 0$), thin solid line = experimentally identified M.T.F.*).

8.2.2. Phase of the total shaking table transfer function (P.T.F.)

Figures 12(b), (d) and (f) compare the experimentally identified phase of the total shaking table transfer function with the analytical predictions obtained using zero and non-zero servovalve time delay, respectively. The quality of the agreement between analytical and experimental results is very similar to that described in Sec. 8.1 assuming perfectly rigid payloads, except for a peak at about 55 Hz predicted by the analytical shaking table model with finite stiffness modelling of the “rigid” payload. This peak, however, is not clearly identified experimentally.

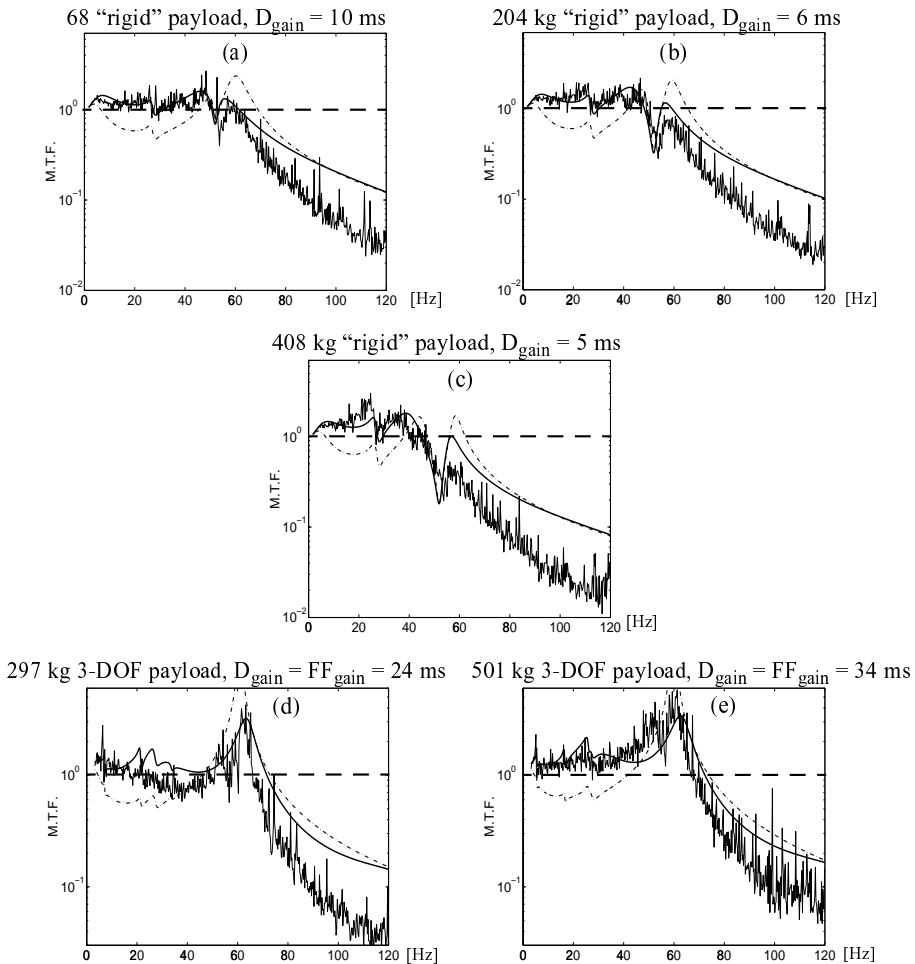


Fig. 14. Magnitude of total shaking table transfer function for the “optimum” control gain setting under various payload conditions; (a), (b), (c): “rigid” payloads of 68, 204, and 408 kg (150, 450 and 900 lbs) with partially flexible analytical modelling; (d), (e): flexible 297 and 501 kg (654 and 1104 lbs) 3-DOF payloads (*thick solid line = analytical M.T.F. with non-zero servovalve time delay τ , dashed dot line = analytical M.T.F. with zero servovalve time delay ($\tau = 0$), thin solid line = experimentally identified M.T.F.*).

8.3. Flexible payload (3-DOF)

Figures 13 and 14 compare the experimentally identified and analytically predicted total shaking table transfer functions for bare table condition (recalled here) and two (flexible) 3-DOF payloads of 297 and 501 kg (654 and 1104 lbs), respectively. The 3-DOF payloads considered consist of a one fifth scale model of a three-storey one bay by one bay steel moment resisting building frame. This physical model is 2.286 m (7.5 ft) tall, 1.37 m (54 in) wide and 0.66 m (26 in) deep and has a dead weight (frame only) of 92.5 kg (204 lbs). It was loaded with two different sets of 68 kg (150 lbs) concrete blocks (“rigidly” attached to the three floors) in order to simulate two 3-DOF payloads of total weight equal to 297 and 501 kg (654 = 204 + 450 lbs and 1104 = 204 + 900 lbs), respectively. The dynamic characteristics (stiffness and mass matrices, natural frequencies and mode shapes) to be included in the analytical shaking table model^y were derived using the CAL-91 computer program [Wilson, 1991] starting from a 3D frame model and performing static condensation to model only the three translational (horizontal) degrees of freedom in the weak direction of the frame model as non-zero mass (dynamic) degrees of freedom. The analytical stiffness and mass matrices obtained are given below and the corresponding first three modal frequencies of vibration are summarized in Table 4 where they are compared with experimentally identified results (obtained using low amplitude white noise excitation in conjunction with transfer function analysis).^z For the sake of consistency with a purely predictive analytical shaking table model, an assigned modal damping ratio of 0.02 (realistic) was used in the shaking table model for all three modes of vibration of the payload.

Stiffness matrix : [K]

$$= \begin{bmatrix} 28.377 (16, 198) & -15.136 (-8, 640) & 1.766 (1, 008) \\ -15.136 (-8, 640) & 26.075 (14, 884) & -12.869 (-7, 346) \\ 1.7661 (1, 008) & -12, 869 (-7, 346) & 11.254 (6424) \end{bmatrix} \begin{matrix} \text{kN/cm} \\ (\text{lbs/in}) . \end{matrix}$$

Mass matrix for the 297 kg (654 lbs) building model:

$$[M] = \begin{bmatrix} 101.3 (0.578) & 0 & 0 \\ 0 & 101.3 (0.578) & 0 \\ 0 & 0 & 94.1 (0.537) \end{bmatrix} \text{kg (lbs s}^2/\text{in)} .$$

^yFor the sake of conciseness, the analytical shaking table model for 2D MDOF payload is not reported in Sec. 3, but is fully described in an earlier publication by the authors [Conte and Trombetti, 2000]. Furthermore, the set of servo-hydraulic parameters used in the analytical model with MDOF payload is the one referred to as “**pf**” in Table 2, while the set of servo-hydraulic parameters referred to as “**d18**” in Table 2 is used in the analytical model for bare table condition. The former set “**pf**” of servo-hydraulic parameters is used because it least-square fits the experimentally identified M.T.F. of the shaking table loaded with a relatively flexible payload (natural frequencies below 50 Hz).

^zFor the detailed description and the analytical and experimental dynamic analyses of these reduced-scale models, the interested reader is referred to Appendix B of the original reports by the authors [Trombetti *et al.*, 1997a].

Table 4. Experimentally derived versus analytically predicted payload natural frequencies.

Vibration Mode	297 kg (654 lbs)	297 kg (654 lbs)	501 kg (1104 lbs)	501 kg (1104 lbs)
	Experimental Natural Frequency (Hz)	CAL 90 Model Natural Frequency (Hz)	Experimental Natural Frequency (Hz)	CAL 90 Model Natural Frequency (Hz)
1st lateral	6.40	7.22	5.15	5.53
2nd lateral	16.82	21.58	13.82	16.60
3rd lateral	22.20	33.86	20.05	26.15

Mass matrix for the 501 kg (1104 lbs) building model:

$$[M] = \begin{bmatrix} 169.4(0.967) & 0 & 0 \\ 0 & 169.4(0.967) & 0 \\ 0 & 0 & 162.2(0.926) \end{bmatrix} \text{ kg (lbs s}^2/\text{in).}$$

8.3.1. Magnitude of the total shaking table transfer function (M.T.F.)

Figures 13(a), (c) and (e) compare the experimentally identified and analytically predicted M.T.F. of the bare table and of the shaking table loaded with either of the two 3-DOF flexible payloads. These plots indicate that the 297 kg (654 lbs) and 501 kg (1104 lbs) frame test models affect the actual shaking table M.T.F. in a similar way, namely:

- Both test specimens give rise to (1) a narrow peak (spike) in the M.T.F. at their first modal (i.e. fundamental) frequency f_1 , and (2) smaller spikes at the higher modal frequencies f_2 and f_3 .
- Both structural models heighten and narrow the oil column peak and slightly lower the oil column frequency. The oil column peak raises from about 1.3 for bare table condition, see Fig. 9(a), to about 2.0 for the 297 kg (654 lbs) specimen and about 3.0 for the 501 kg (1104 lbs) specimen. The oil column frequency decreases from about 70 Hz for bare table condition to approximately 62 Hz for both specimens.
- Both structural specimens decrease, well below unity, the total shaking table M.T.F. in the intermediate frequency range (the M.T.F. decreases to approximately 0.65 in the frequency range between 30 and 50 Hz).

Comparisons between the experimentally identified and analytically derived total shaking table transfer functions show that the analytical model incorporating the servovalve time delay τ has good predictive capabilities, although it overestimates the experimentally identified M.T.F. in the intermediate frequency range (20–50 Hz). In the case of the 501 kg (1104 lbs) test specimen, notice in particular how well the analytical model accounting for servovalve time delay captures (1) the two peak and notch effects (at about 5 Hz and 17 Hz) in the M.T.F. corresponding to the payload first two natural frequencies and (2) the foundation/reaction mass

resonance peak^{aa} (at about 27 Hz), with however some underestimation of the amplitude of the oil column peak. In the case of the 297 kg (654 lbs) payload, notice the small difference between the analytically derived and experimentally observed first modal spike frequency, which is due to the analytical overestimation of the test specimen fundamental frequency (see Table 4). It is also observed that the analytical model accounting for the servovalve time delay captures very well the oil column peak.

8.3.2. *Phase of the total shaking table transfer function (P.T.F.)*

Figures 13(b), (d) and (f) compare the experimentally identified and analytically predicted phase of the total shaking table transfer function (P.T.F.) for the bare table and shaking table loaded with either of the two 3-DOF flexible payloads. Overall, we observe a noticeable increase (as compared to bare table condition) of the phase lag in the frequency range between 0 and 50 Hz for both test specimens.

As shown in Figs. 13(d) and (f), both analytical shaking table models predict small and sharp notches in the shaking table P.T.F. at the locations of the natural frequencies of the test specimen.^{ab} These small distortions in the P.T.F. are very difficult to observe experimentally due to the inherent jaggedness (statistical variability) of the estimated experimental P.T.F. However, Fig. 13(f) shows clearly the notch in both the analytical (with servovalve time delay) and experimental P.T.F.'s due to the first modal (i.e. fundamental) frequency of the test specimen. The analytical model incorporating the servovalve time delay captures better (than the analytical model with zero servovalve time delay) the shape of the experimentally identified P.T.F. in the frequency range between 0 and 20 Hz. It however overestimates the phase lag induced by the shaking table system.

8.4. *Tuning of control gain parameters to compensate for payload effects*

Based on the understanding of the sensitivities of the total shaking table transfer function to the user-set control gain parameters and to the payload characteristics presented in Secs. 6 and 8.1 through 8.3, the control gains were re-tuned in order to re-optimize the dynamic performance of the shaking table system (i.e. bring the magnitude of the total shaking table transfer function closer to unity) under various loading conditions. Figures 14(a), (b) and (c) show the experimentally identified and analytically predicted (with partially flexible payload modelling) magnitude of the total shaking table transfer function for a “rigid” payload of 68, 204, and 408 kg

^{aa}As the third modal frequency of the 501 kg (1104 lbs) test specimen is very close to the foundation/reaction mass resonance frequency, dynamic interaction between both occurs as shown by the analytically predicted M.T.F.

^{ab}It is found analytically that these notches increase in size with the weight of the payload for a fixed set of modal frequencies [Trombetti *et al.*, 1997a].

(150, 450, and 900 lbs), respectively, and for re-tuned^{ac} (re-optimized) control gain parameters. These figures can be compared directly with Figs. 12(a), (c) and (e) which show the shaking table M.T.F. obtained for the same payload conditions, but using the “optimum” control gain setting for bare table condition. The re-optimized control gains are equal to the ones for bare table condition, except for the derivative gain (D_{gain}) which is given in Fig. 14 for each specific payload. Notice the effectiveness of reducing D_{gain} in lowering the shaking table M.T.F. in the intermediate frequency range, thus compensating for the undesirable payload effect. It is worth noting the very good agreement obtained between experimental and analytical (accounting for servovalve time delay) shaking table M.T.F.’s, even though the same set of servo-hydraulic parameters (“**pf**” in Table 2, obtained for $D_{\text{gain}} = 18$ ms) was used for all analytical predictions in Figs. 14(a), (b), and (c).

Similarly, Figs. 14(d) and (e) show the experimental and analytical total shaking table M.T.F.’s for the two flexible 3-DOF payloads of 297 kg (654 lbs) and 501 kg (1104 lbs), respectively, and for re-tuned control gain parameters, while Figs. 13(c) and (e) show the same shaking table M.T.F.’s, but obtained using the “optimum” control gain setting for bare table condition. Only the values of the D_{gain} and FF_{gain} changed during re-tuning as indicated in Figs. 14(d) and (e). Increasing D_{gain} and FF_{gain} proved effective in providing the needed raise of the shaking table M.T.F. in the intermediate frequency range, but simultaneously amplified the oil column peak. Notice the good predictive capability of the analytical shaking table model (incorporating the servovalve time delay), except for some overestimation of the M.T.F. in the intermediate frequency range for the 297 kg (654 lbs) test specimen and some misfit^{ad} in the oil column frequency region for the 501 kg (1104 lbs) test specimen (overestimation of the oil column frequency). The effects of the five control gain parameters on the magnitude of the analytical transfer function of the shaking table — payload system are represented synoptically in Figs. 15 and 16 as a guidance on control gain adjustments for future experiments. The range of adjustment of the control gain parameters is limited by stability constraints of the control system.

In summary, the test-analysis correlation study for different payload conditions presented in Secs. 8.1–8.4 reveals that (1) a payload (even as low as 10 percent of the table maximum payload capacity) does affect significantly the total shaking table transfer function, and (2) the control gain parameters can be used to effectively compensate in part for these payload effects. Overall, the linear analytical model of the shaking table system, which incorporates the servovalve time delay, is proven to

^{ac}The systematic procedure followed to re-optimize the user-set control gains for a specific payload condition is described in detail in the original report by the authors [Trombetti *et al.*, 1997b].

^{ad}This mis-prediction can be attributed to the following two factors: (1) the values of D_{gain} and FF_{gain} are relatively far from the linearisation point ($D_{\text{gain}} = FF_{\text{gain}} = 18$ ms) used to obtain the set of servo-hydraulic parameters (“**pf**”) adopted in this analytical prediction, and (2) unmodelled high frequency dynamics due to the clamping system used to attach the concrete blocks at the floor levels of the steel frame model.

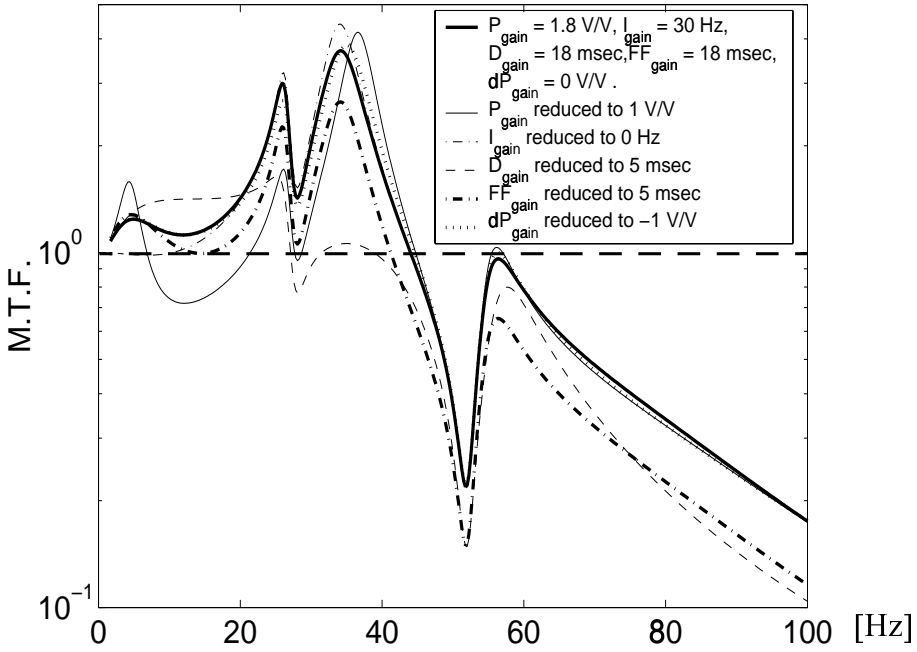


Fig. 15. Sensitivity of analytical total shaking table transfer function to control gain parameters for table loaded with 297 kg (654 lbs) "rigid" payload.

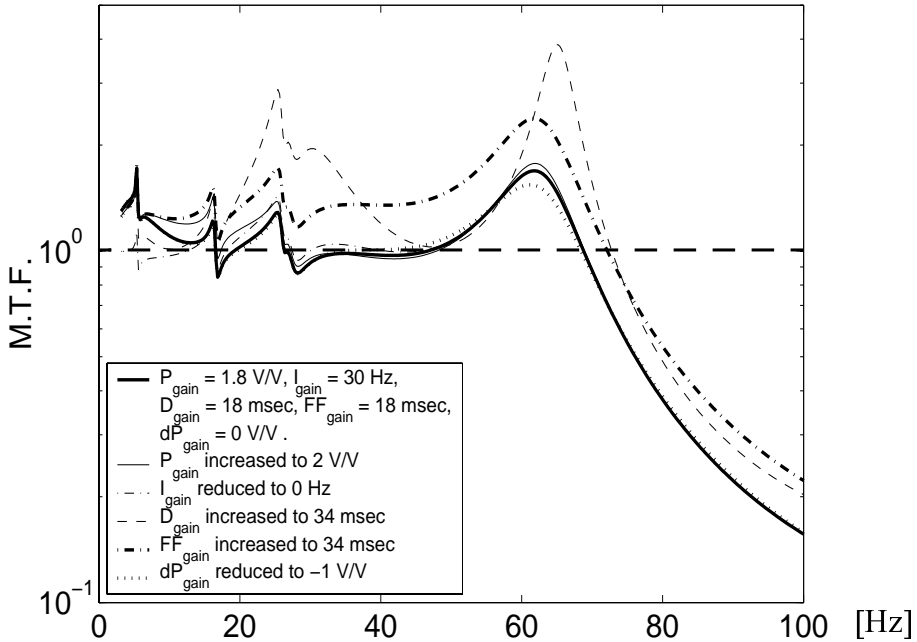


Fig. 16. Sensitivity of analytical total shaking table transfer function to control gain parameters for table loaded with 501 kg (1104 lbs) 3-DOF payload.

have very good predictive capabilities over a wide range of operating and payload conditions.

9. Conclusions

This paper focuses on a comprehensive test-analysis comparison study of shaking table dynamics and how the table dynamic performance is affected by various operating and payload conditions. The successful results obtained contribute (1) to validate the linear analytical model previously developed by the authors from basic physical principles, which accounts for servovalve-actuator-control-foundation-specimen interaction, and (2) to shed light into the understanding of the dynamic behavior of a small-to-medium size, uni-axial, servo-hydraulic, displacement-controlled shaking table system and its governing parameters.

It was observed that the analytical shaking table model used herein, which is obtained by linearising the inherently nonlinear servo-hydraulic shaking table system about only a few operating points, has very good predictive capabilities over a wide range of operating and payload conditions. This provides a clear indication of the robustness of the model and suggests that a reliable method to model the dynamic performance of shaking table systems of the class considered here is achieved within the limitations of a linear elastic test specimen and a servo-hydraulic system performing within (and not close to or on) its performance envelope. The inclusion of the servovalve time delay in the analytical shaking table model (a unique feature of the model) proved essential to achieve the reliable analytical predictions obtained.

It is found both analytically and experimentally that the presence of a payload may significantly affect the total shaking table transfer function. Nonetheless, it was seen that the user-set control gain parameters (proportional, integral, derivative, feedforward, and differential pressure) are capable of compensating in part for these payload effects. The analytical shaking table model developed and calibrated to the Rice University shaking table proved invaluable in understanding the sensitivities of the total shaking table transfer function to the various control gain parameters. These sensitivities were successfully used to identify the set of control gain parameters that optimizes the shaking table reproduction of a target strong motion record for a given payload condition.

Also provided in this paper is a noteworthy example of the power of an integrated approach of physical experimentation and physics-based analytical modelling and prediction in leading to the proper physical understanding of experimental shaking table results, which would not have been possible using either approach in isolation.

Acknowledgements

The support of the National Science Foundation under Grant No. BCS-9311031 and matching funds from Rice University for the design, analysis and construction

of a medium-size shaking table system are gratefully acknowledged. The authors wish to thank Prof. A. J. Durrani, Chairman of the Civil Engineering Department at Rice University, for his support and insightful suggestions provided in the course of this study.

References

- Bartlett, M. S. [1948] "Smoothing periodograms from time series with continuous spectra," *Nature* **161**, 686–687.
- Bode, H. W. [1965] "Feedback: the history of an idea," *Conference on Circuits and Systems*, New York, John Wiley.
- Carydis, P. G. *et al.* [1995] "Comparative shaking table studies at the National University of Athens and at Bristol University," *Proc. 10th European Conf. on Earthquake Engineering*, Vienna, 1994, pp. 2993–2997.
- Clark, A. [1992] "Dynamic Characteristics of large multiple degree of freedom shaking tables," *Proc. 10th World Conf. on Earthquake Engineering*, Madrid, Spain, pp. 2823–2828.
- Conte, J. P. and Trombetti, T. L. [2000] "Linear dynamic modeling of a uni-axial servo-hydraulic shaking table system," *Earthq. Engrg. Struct. Dyn.* **29**(9), 1375–1404.
- Crewe, A. J. and Severn, R. T. [2001] "The European collaborative programme on evaluating the performance of shaking tables," *Phil. Trans. Roy. Soc. London* **359**, 1671–1696.
- Dyke, S. J., Spencer, Jr., B. F., Quast, P. and Sain, M. K. [1995] "Role of control-structure interaction in protective system design," *J. Engrg. Mech. ASCE* **121**(2), 322–338.
- Franklin, G. F., Powell, J. D. and Emami-Naeini, A. [1994] *Feedback Control of Dynamic Systems*, Third Edition, Addison-Wesley.
- Hwang, J. S., Chang, K. C. and Lee, G. C. [1987] "The system characteristics and performance of a shaking table," *NCEER Report No. 87-0004*, National Center for Earthquake Engineering Research, State University of New York at Buffalo, New York, USA.
- Kusner, D. A., Rood, J. D. and Burton, G. W. [1992] "Signal reproduction fidelity of servo-hydraulic testing equipment," *Proc. 10th World Conf. on Earthquake Engineering*, Madrid, Spain, pp. 2683–2688.
- Lin, Y. K. [1986] *Probabilistic Theory of Structural Dynamics*, R. E. Krieger Publ. Company, Original Ed., 1967, Reprint 1976, with corrections, 1986.
- Matlab* [1992] *High-Performance Numeric Computation and Visualization Software*, User's Guide, The MathWorks, Inc., Natic, Massachusetts, USA.
- Muhlenkamp, M., Conte, J. P., Hudgings, T. R. and Durrani, A. J. [1997] "Analysis, design, and construction of a shaking table facility," *Structural Research at Rice, Report No. 46*, Department of Civil Engineering, Rice University, Houston, Texas, USA.
- Rea, D., Abedi-Hayati, S. and Takahashi, Y. [1977] "Dynamic analysis of electro-hydraulic shaking tables," *EERC Report No. 77/29*, Earthquake Engineering Research Center, University of California at Berkeley, California, USA.
- Rinawi, A. M. and Clough, R. W. [1991] "Shaking table-structure interaction," *EERC Report No. 91/13*, Earthquake Engineering Research Center, University of California at Berkeley, California, USA.
- Stoten, D. P. and Gomez, E. G. [2001] "Adaptive control of shaking tables using the minimal control synthesis algorithm," *Phil. Trans. Roy. Soc. London* **359**, 1697–1723.

- Trombetti, T. L., Conte, J. P. and Durrani, A. J. [1997a] "Analytical modeling of a shaking table system," *Structural Research at Rice, Report No. 48*, Department of Civil Engineering, Rice University, Houston, Texas, USA.
- Trombetti, T. L., Conte, J. P. and Durrani, A. J. [1997b] "Correlation studies between analytical and experimental dynamic behavior of the Rice University shaking table," *Structural Research at Rice, Report No. 49*, Department of Civil Engineering, Rice University, Houston, Texas, USA.
- Wilson, E. L. [1991] "CAL-91 — Computer Assisted Learning of Static and Dynamic Analysis of Structural Systems," *Report No. UCB/SEMM-91/01*, Department of Civil Engineering, University of California, Berkeley, California, USA.